

**Synthesis of Perylenediimide and Fullerene  
Functionalized Molecular Glasses**

**Synthèse de verres moléculaires fonctionnalisés  
avec des pérylènediimides et des fullerènes**

A Thesis Submitted to the Division of Graduate Studies  
of the Royal Military College of Canada

by

**Zahra Ghoshouni Rahami**

In Partial Fulfillment of the Requirements for the Degree of

Master of Science

September, 2014

© Copyright for open publication remains the property of the author

## **Statement of Originality**

I hereby certify that all of the work described within this thesis is the original work of the author. Any published (or unpublished) ideas and/or techniques from the work of others are fully acknowledged in accordance with the standard referencing practices.

## **Acknowledgments**

I would like to express my deepest appreciation for the feedback, advice, and guidance of my thesis supervisor Professor Olivier Lebel. I would also like to thank him not only for his insight and intuition but also for his encouragement that helped make years of research enjoyable. My greatest appreciation is extended to Lebel group members especially Dr. Tayel Al Hujran for many productive discussions over the past two years.

I would like to offer my thanks to chemistry department technologists especially Dr. Neda Bavarian, Bob Whitehead and John Perreault for their assistance in the analysis phase of the project. In addition I had the great privilege to find many good friends in graduate students' community of RMC during my Masters's study. I also acknowledge the financial support provided by DRDC during the course of this project.

The last but certainly not least, I would like to express my gratitude and thanks to my husband and my parents whose encouragement and support were always invaluable to me, and in fact the love and support offered by them kept me going throughout the process of researching and writing this thesis.

## **Abstract**

Organic molecular glasses are considered as an important category of organic functional materials that have attracted increasing attention in technical applications. The ability of these compounds to produce amorphous uniform thin films that are easy to process, makes them appealing candidates as chromophores, semiconductors and charge transport materials in several fields such as organic electronics, optoelectronics, and photonics. The advantages associated with these amorphous molecular materials, such as small size and low molecular weight, make the process of characterization and purification easier. In our research group, molecular glasses functionalized with selected electron transporting groups have been designed, synthesized, and characterized. Also corresponding molecular and physical properties have been investigated by DSC (differential scanning calorimetry) and UV-Vis spectroscopy. In this research thesis strategies to design and synthesize glasses functionalized with perylene diimide (PDI) dyes and fullerenes and corresponding properties will be discussed

## Résumé

Les verres moléculaires organiques sont une famille importante de matériaux fonctionnels organiques qui ont suscité beaucoup d'intérêt pour certaines applications techniques. La capacité de ces composés de former des couches minces amorphes uniformes qui sont faciles à mettre en oeuvre fait de ces matériaux des candidats idéaux comme chromophores, semiconducteurs ou transporteurs de charge dans des domaines tels que l'électronique organique, l'optoélectronique et la photonique. La petite taille et la basse masse moléculaire de ces composés leur procure des avantages au niveau de la purification et de la caractérisation. Dans notre groupe de recherche, nous avons conçu, synthétisé et caractérisé des verres moléculaires fonctionnalisés avec des groupes transporteurs d'électrons. De plus, nous avons déterminé leurs propriétés physiques à l'aide de la calorimétrie différentielle à balayage (DSC, *differential scanning calorimetry*) et la spectroscopie UV-Visible. Le but principal de cette thèse est de discuter des nouvelles stratégies mises au point pour la conception et la synthèse de verres moléculaires fonctionnalisés avec des colorants pérylènediimides (PDI) et des fullerènes.

## Table of Contents

Statement of Originality.....	ii
Acknowledgments.....	iii
Abstract.....	iv
Résumé.....	v
List of Figures.....	viii
List of Tables.....	ix
List of Schemes.....	ix
List of Abbreviation.....	x
<b>1 Introduction.....</b>	<b>1</b>
1.1. Background.....	1
1.1.1. Definition of Molecular Glasses.....	2
1.1.1.1. Natural Molecular Glasses.....	2
1.1.1.2. Synthetic Molecular Glasses.....	2
1.1.1.2.1. Star-shaped $\pi$ -Conjugated Based Molecular Glasses.....	3
1.1.1.2.2. Mexylamine Triazine Based Molecular Glasses.....	8
1.1.1.2.2.1. The Influence of the Head Group.....	8
1.1.1.2.2.2. The Influence of the Tail Group.....	10
1.1.1.2.2.3. Mexylaminotriazine Functionalized Dyes.....	12
1.2. Applications of Molecular Glasses.....	14
1.2.1. Pharmaceutical Glasses.....	15
1.2.2. Electronic and Optoelectronic Applications.....	15
1.2.2.1. Organic Light Emitting Diodes (OLEDs).....	16
1.2.2.2. Organic Photovoltaic Devices (OPVs).....	18
1.2.2.3. Organic Field Effective Transistors (OFETs).....	20
1.2.3. Photochromic Amorphous Molecular Glasses.....	21
1.2.4. Nanolithography Applications.....	23
1.3. Statement of Research Objectives.....	25
<b>2 PDI-Functionalized Molecular Glasses.....</b>	<b>26</b>
2.1. Introduction.....	26
2.1.1. Definition and Properties of PDI dyes.....	26
2.1.2. Applications.....	26
2.1.3. Potential Applications of PDI-Functionalized Molecular Glasses.....	27
2.2. Results and Discussion.....	27

2.2.1. Synthesis and Characterization .....	33
2.2.2. Optical properties.....	38
2.2.3. Thermal Properties.....	38
2.2.4. Photovoltaic Properties .....	39
2.3. Experimental .....	42
2.3.1. Material and Equipments .....	42
2.3.2. Synthesis .....	42
2.3.2.1. Synthesis of Compound <b>59</b> .....	42
2.3.2.2. Synthesis of Compound <b>60</b> .....	43
2.3.2.3. Synthesis of Compound <b>61</b> .....	43
2.3.2.4. Synthesis of Compound <b>62</b> .....	44
2.3.2.5. Synthesis of Compound <b>63</b> .....	45
2.4. Summary .....	45
2.5. Appendix.....	45
2.5.1. NMR Figures .....	45
2.5.2. DSC Thermograms .....	50
<b>3 Fullerene-Functionalized Molecular Glasses.....</b>	<b>52</b>
3.1. Introduction.....	52
3.1.1. Definition and Properties of Fullerene Dyes.....	52
3.1.2. Applications .....	52
3.1.3. Potential Applications of Fullerene Functionalized Molecular Glasses .....	52
3.2. Results and Discussion .....	53
3.2.1. Synthesis and Characterization .....	54
3.3. Experimental .....	55
3.3.1. Material and Equipment.....	55
3.3.2. Synthesis .....	55
3.3.2.1. Attempted Synthesis of Compound <b>66</b> .....	56
3.3.2.2. Attempted Synthesis of Compound <b>68</b> .....	56
3.3.2.3. Attempted Synthesis of Compound <b>72</b> .....	56
3.4. Summary .....	57
3.5. Appendix.....	58
3.5.1. NMR spectra .....	58
<b>4 Conclusion and Future Goals.....</b>	<b>60</b>
Bibliography .....	62

## List of Figures

Figure 1: A) Fully spiro-configured terfluorene compounds and related molecular design concept. B) molecular structure taken from molecular calculations using the Amber software. ....	5
Figure 2: The photovoltaic process: absorption of photons (A) generation of carriers (G), collection of carriers (C). <sup>39</sup> .....	18
Figure 3: Thin films of PDI-functionalized molecular glasses prepared by spin-coating from CH <sub>2</sub> Cl <sub>2</sub> or THF solution. From left to right: <b>61</b> , <b>62</b> , <b>60</b> . ....	35
Figure 4: UV-Vis absorption spectra of PDI-functionalized molecular glasses in CH <sub>2</sub> Cl <sub>2</sub> solution.....	36
Figure 5: UV-Vis absorption spectra of PDI-functionalized molecular glasses deposited from CH <sub>2</sub> Cl <sub>2</sub> or THF as thin films. ....	36
Figure 6: I-V curves of photovoltaic cells of compound <b>61</b> with P <sub>3</sub> HT obtained from three different ratios (2:1, 1:1, 1:2). ....	40
Figure 7: I-V curves of photovoltaic cells of compound <b>62</b> with P <sub>3</sub> HT. ....	41
Figure 8: <sup>1</sup> H NMR spectrum of compound <b>59</b> , in CDCl <sub>3</sub> , 300 MHz. ....	46
Figure 9: <sup>1</sup> H NMR spectrum of compound <b>60</b> in DMSO- <i>d</i> <sub>6</sub> , 400 MHz. ....	46
Figure 10: <sup>1</sup> H NMR spectrum of compound <b>61</b> in DMSO- <i>d</i> <sub>6</sub> , 400 MHz. ....	47
Figure 11: <sup>1</sup> H NMR spectrum of compound <b>62</b> in DMSO- <i>d</i> <sub>6</sub> , 400 MHz. ....	47
Figure 12: <sup>1</sup> H NMR spectrum of compound <b>63</b> in DMSO- <i>d</i> <sub>6</sub> , 400 MHz. ....	48
Figure 13: <sup>13</sup> C NMR spectrum of compound <b>60</b> in DMSO- <i>d</i> <sub>6</sub> , 75 MHz. ....	48
Figure 14: <sup>13</sup> C NMR spectrum of compound <b>61</b> in DMSO- <i>d</i> <sub>6</sub> , 75 MHz. ....	49
Figure 15: <sup>13</sup> C NMR spectrum of compound <b>62</b> in DMSO- <i>d</i> <sub>6</sub> , 75 MHz. ....	49
Figure 16: DSC analysis of compound <b>60</b> . ....	50
Figure 17: DSC analysis of compound <b>61</b> . ....	50
Figure 18: DSC analysis of compound <b>62</b> . ....	51
Figure 19: <sup>1</sup> H NMR spectrum of compound <b>66</b> in THF, 400 MHz, before purification on preparative TLC plate. ....	58
Figure 20: <sup>1</sup> H NMR spectrum of compound <b>66</b> in THF, 400 MHz, after purification on preparative TLC plate. ....	58
Figure 21: <sup>1</sup> H NMR spectrum of compound <b>72</b> in THF, 400 MHz, before purification on preparative TLC plate. ....	59
Figure 22: <sup>1</sup> H NMR spectrum of compound <b>72</b> in THF, 400 MHz, after purification on preparative TLC plate. ....	59

## List of Tables

Table 1: Temperatures of glass-transition ( $T_g$ ), crystallization ( $T_c$ ), and melting ( $T_m$ ) for star-shaped compounds <b>1-19</b> . .....	7
Table 2: UV-Vis absorbance values of PDI functionalized molecular glasses in solution and in the solid state. ....	37
Table 3: Photovoltaic parameters of photovoltaic cells of compound <b>61</b> with P3HT. ....	40
Table 4: Photovoltaic parameters of photovoltaic cells of compound <b>62</b> with P3HT. ....	41

## List of Schemes

Scheme 1: Triazine glass with two tail groups and one head group. ....	8
Scheme 2: Mexylaminotriazine glass. ....	10
Scheme 3: Synthesis of mexylaminotriazine glasses. ....	12
Scheme 4: Synthesis of molecular glass <b>27</b> . ....	13
Scheme 5: Synthesis of molecular glass <b>31</b> . ....	14
Scheme 6: Ring closure-ring opening reaction of TPTTC upon irradiation with UV-light. ....	22
Scheme 7: Ring closure-ring opening reaction of BMSO upon irradiation with UV-Vis light. ....	23
Scheme 8: Synthesis of compound <b>58</b> . ....	28
Scheme 9: Synthesis of compound <b>59</b> . ....	28
Scheme 10: Synthesis of compound <b>60</b> . ....	29
Scheme 11: Synthesis of compound <b>61</b> . ....	30
Scheme 12: Synthesis of compound <b>62</b> . ....	31
Scheme 13: Synthesis of compound <b>63</b> . ....	32
Scheme 14: P3HT used as donor polymer in photovoltaic cell. ....	39
Scheme 15: Synthesis of compound <b>66</b> . ....	53
Scheme 16: Synthesis of compound <b>68</b> . ....	53
Scheme 17: Synthesis of compound <b>72</b> . ....	54

## List of Abbreviations

**Ad(tBuSSB)<sub>4</sub>**: Tetrakis(4-*tert*-butylstyrylstilbenyl)adamantane

**ASITPA**: 4, 4', 4''-Tris(allylsuccinimido)triphenylamine

**BHJ**: Bulk heterojunction

**BMSO**: 5-[Bis(4-methyl-phenyl)amino]-1,2,3-trimethylspiro{indoline-2,3'-(3H-naphth[2,1b][1,4]oxazine)}

**CDI**: Carbonyldiimidazole

**CTAB**: Cetrimonium bromide

**CuPc**: Copper phthalocyanine

**C(tBuSSB)<sub>4</sub>**: Tetrakis(4-*tert*-butylstyrylstilbenyl) methane

**DCM**: Dichloromethane

**DEH**: 4-Diethylaminobenzaldehyde diphenyl- hydrazine

**DIBAL**: Diisobutylaluminum hydride

**DMF**: Dimethyl formamide

**DMSO**: Dimethylsulfoxide

**DPH**: 4-Diphenylaminobenzaldehyde diphenylhydrazone

**DR1**: Disperse Red 1

**DSC**: Differential scanning calorimetry

**EL**: Electroluminescence

**EtOAc**: Ethyl acetate

**FF**: Fill factor

**FTIR**: Fourier transform infrared spectroscopy

**HOMO**: Highest occupied molecular orbital

**HRMS** : High resolution mass spectroscopy

**ISC**: Short circuit current

**ITO**: Indium tin oxide

**J<sub>sc</sub>**: Short circuit current

**LER**: Line edge roughness

**LUMObfcta**: Lowest unoccupied molecular orbital

**M-DPH**: 4-Diphenylaminoacetophenone diphenylhydrazone

**MTDAPB** : Methyl-1,3,5-tris[4-(diphenylamino)phenyl]benzene

**NEt<sub>3</sub>**: Triethylamine

**NMR** : Nuclear magnetic resonance  
**OFET**: Organic field-effect transistors  
**OLED**: Organic light-emitting diodes  
**OPV**: Organic photovoltaic  
**PAG**: Photoacid generator  
**PCBM**: Phenyl-C61-butyric acid methyl ester  
**PCE**: Power conversion efficiency  
**PDI**: Perylene diimide  
**PEDOT**: Poly(3,4-ethylenedioxythiophene)  
**PGMEA**: Propylene glycol methyl ethyl acetate  
**P3HT**: Poly (3-Hexylthiophene)  
**PSS**: Poly (styrenesulfonate)  
**ppm**: Parts per million  
**R<sub>s</sub>**: Series resistance  
**R<sub>SH</sub>**: Shunt resistance  
**rt**: Room temperature  
**Si(tBuSSB)4**: Tetrakis(4-tert-butylstyrylstilbenyl)silane  
**TBA**: Tri(biphenyl-4-yl)amine  
**TBPhB**: Tris(2,3,5,6-tetramethylbiphenyl-4-yl) borane  
**t-BuBBAB**: 4,4'-Bis[bis(4'-tert-butylbiphenyl-4-yl)amino]azobenzene  
**TDAB** : 1,3,5-Tris(diphenylamino)benzene  
**TDAPB**: 1,3,5-Tris[4-(diphenylamino)phenyl]benzene  
**TDATA** : Tris(diphenylamino)- triphenylamine triarylamine  
**TFT**: Thin film transistors  
**T<sub>g</sub>**: Glass transition temperature  
**THF**: Tetrahydrofuran  
**TPA**: Triphenylamine  
**TPhB**: Tris(2,3,5,6-tetramethylphenyl) borane  
**TPP**: Tetraphenylporphyrin  
**TP TTC**: 1-{5-[4-(Di-p-tolylamino)phenyl]-2-methylthiophen-3-yl}-2-(2,5-dimethylthiophen-3-yl)-3,3,4,4,5,5-hexafluorocyclopentene  
**TTA**: Tri(p-terphenyl-4-yl)amine  
**TTPhB**: Tris(2,3,5,6-tetramethyl-1,1';4',1''terphenyl-4-yl) borane  
**TTPhPhB**: Tris[4-(1,1';3',1''-terphenyl-5'-yl)-2,3,5,6-tetramethylphenyl]borane  
**TLC**: Thin layer chromatography  
**TsOTPB**: 1,3,5-Tris[4-(4-toluenesulfonyloxy)phenyl]benzene  
**UV-Vis**: Ultraviolet-visible

**V<sub>oc</sub>**: Open circuit voltage

**ZnO**: Zinc oxide

# 1 Introduction

## 1.1. Background

Thin film technology has progressed dramatically during the past four decades. In this process, a thin layer of material, ranging from nanometers (monolayer) to micrometers in thickness is deposited on a flat surface. These deposited thin films have several applications such as electronic components, optical coatings, magnetic films for storage, optical data storage devices, antistatic coatings and hard space coatings.<sup>1</sup>

The materials used to prepare thin films cover a wide range of inorganic, organometallic and organic compounds.<sup>1</sup> However the two main classes of materials used to form amorphous thin films are polymers (organic and inorganic materials) and small molecules. Polymers and composite polymers are capable of forming high quality amorphous films. However, the properties associated with these candidates, such as large molecular size and polydispersity, make the synthesis, purification and characterization of these compounds difficult, and their composition is not homogeneous from one sample to another.<sup>2</sup> In addition, it is challenging to synthesize and process inorganic polymer based thin films due to the low solubility of inorganic materials. Metal oxide thin films, such as ZnO, need to be annealed as deposited to form uniform thin films.<sup>3</sup>

In comparison to polymers, small molecules benefit from generally easier synthesis and characterization, and higher consistency between different samples. However, with such molecules, thin film quality is typically inferior (e.g. films are less uniform, more grainy) and there is an increased tendency for small molecules to crystallize. In contrast to materials discussed above, molecular glasses are small molecules with discrete molecular structures that are capable of forming uniform amorphous phases.<sup>2</sup>

Due to properties explained above, molecular glasses are considered an alternative to polymers in the field of thin film technology, possessing a desirable ensemble of advantages from both polymers and small molecules. Nevertheless, there are some limitations associated with such molecules, such as (1) the tendency of molecular glasses, like all small molecules, to readily revert to the thermodynamically more stable crystalline state, (2) accessing the glassy state that is often only possible through special processing techniques such as super-cooling and freeze-drying, and (3) the current design of structures that will result in glass formation which relies mostly on trial and error.<sup>4</sup>

### **1.1.1. Definition of Molecular Glasses**

Low molecular weight organic compounds capable of forming stable solid amorphous phases are called amorphous molecular materials, low molar mass glasses or molecular glasses. A glass can be defined as a type of solid in which atom arrays are disordered and contain many internal degrees of freedom. The environment of atoms in a glass is similar to the atoms in a crystal in terms of distance and the number of neighbors although a glass, unlike a crystal, lacks long-range molecular arrangements and positional and directional ordering.<sup>5</sup>

#### **1.1.1.1. Natural Molecular Glasses**

The amorphous phase is the most common form of certain natural materials such as proteins, peptides and some sugars.<sup>6</sup> Among natural glass-forming materials, sugars have received the attention of researchers. The glass-forming ability of sugars is important for several reasons: Sugar glasses such as sucrose and trehalose are effective materials in protecting numerous organisms in dry or cold conditions for extended periods of times.<sup>7</sup>

In dehydrated conditions, sugars form glasses to protect cells from denaturation and formation of molecular aggregates.<sup>7</sup> In addition, disaccharides can be used as glassy matrices to stabilize proteins and cell components for spectroscopic studies.<sup>8</sup> The glass transition in sugars is also important in the food industry. For example, the texture of candies and cookies depends on the glass transition temperature and degree of crystallinity of sugar mixtures.<sup>9</sup>

Other naturally occurring glasses are mineral glasses. The structural investigation classified volcanic glasses in two groups of more ordered silica-like glasses (Fulgurite, Wabar glass, Lechatelierite, Libyan desert glass), and silica glasses possessing less ordered structures, including Macusani glass (Peru) and obsidians from Lipari Island (Italy) and Kenya.<sup>10</sup> These glasses are mainly composed of silica but contain minor impurities such as  $\text{Al}_2\text{O}_3$ ,  $\text{B}_2\text{O}_3$ ,  $\text{MgO}$  and  $\text{P}_2\text{O}_5$ .

#### **1.1.1.2. Synthetic Molecular Glasses**

In this section, recent studies on the design of glass-forming molecular structures will be explained. Also, the correlation between molecular structure, glass transition temperature and amorphous phase stability for these materials will be discussed.

In order to facilitate the formation of amorphous phases and prevent crystallization, substituents with specific characteristics should be introduced in the

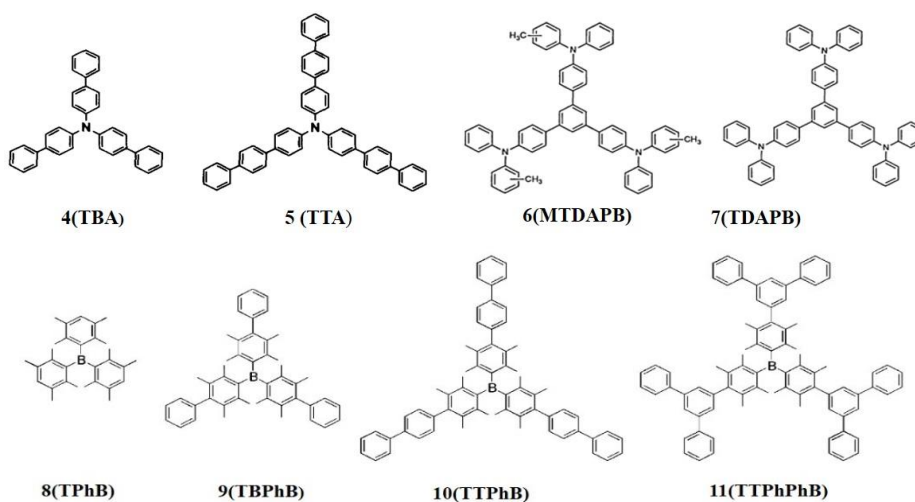
molecular skeleton of compounds to induce irregular structures. The important parameter to favor amorphous phase formation is the shape of the molecule.<sup>11</sup> Strategies to create proper shapes rely on designing structures that are considered difficult to pack and crystallize. Guidelines are based on principles such as increasing the number of conformations, reducing symmetry, integrating long and often branched alkyl chains, and generating globular shapes.<sup>12</sup> Based on this idea, the concept of  $\pi$ -electron starburst molecule was proposed by Shirota for the design of amorphous molecular materials.<sup>11</sup> Several families of organic  $\pi$ -electron systems have been synthesized which will be described in the following sections.

### 1.1.1.2.1. Star-shaped $\pi$ -Conjugated Based Molecular Glasses

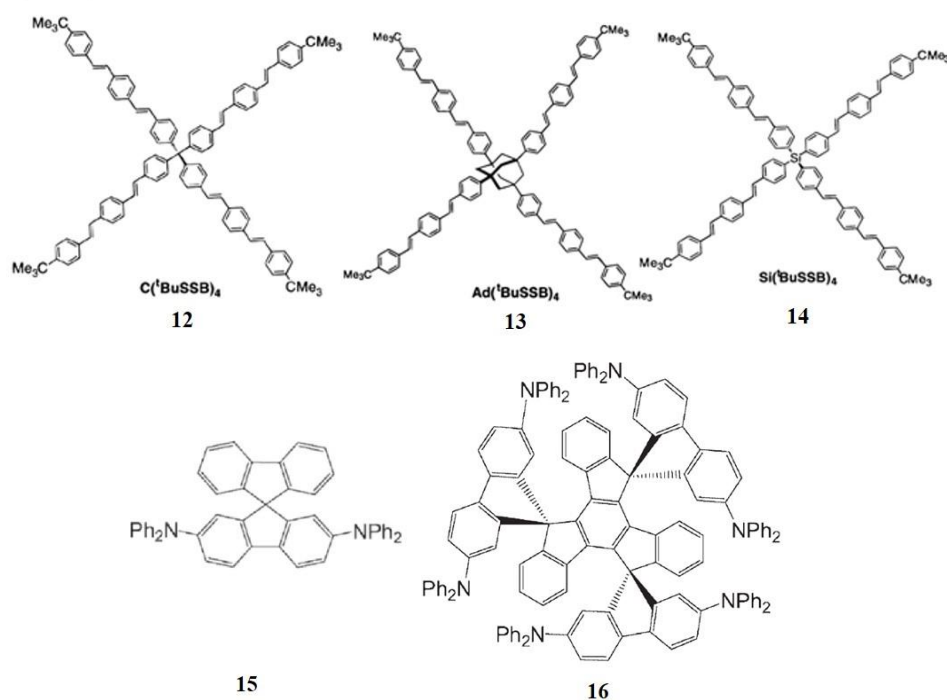
Several classes of amorphous molecular materials have been designed and synthesized by Shirota *et. al.* based on star-shaped molecular structures.<sup>13, 14, 15, 16</sup>



These families of molecular glasses are based on aryl hydrazones (**1-3**),<sup>13</sup> triphenylamine/triphenylbenzene (**4-7**),<sup>14,15</sup> and triphenylborane (**8-11**).<sup>16</sup> As the parent compounds readily crystallize, these glass-forming compounds are functionalized with conjugated arms which give the molecules their distinct star shapes



The presence of conjugated arms surrounding the molecule is a common feature in this family of materials, but the central junction to which the conjugated arms are connected can adopt other geometries such as tetrahedral or spiro-shaped (**12-19**). Compounds with a single central spirocyclic system (**15**), and compounds with several peripheral spirocyclic groups have been synthesized based on spirobifluorene with conjugated substituents and free rotating diphenylamino groups (**16**).<sup>18</sup> and spirobifluorene derivative **19**, which contains dendritic spiro substituents<sup>19</sup>, presents the highest  $T_g$  in the whole group.



The aforementioned star-shaped derivatives were synthesized either by substitution or coupling reactions starting from simple precursors which are usually incapable of forming glassy phases. In order to prevent close packing and induce amorphous phase formation, various strategies have been applied to design the structures.

As shown in Table 1, hydrazones **1-3** show the lowest  $T_g$  among the compounds previously introduced and triphenylamine, triphenylbenzene and triphenylborane-based compounds (**4-11**) present higher  $T_g$  compared to the category of aryl hydrazones (**1-3**). Incorporation of small  $\pi$ -conjugated systems

around a core incapable of making glassy phases results in compounds capable of glass formation; however, such glasses present the low  $T_g$  and are not very stable. The amorphous phase for the case of **1** is only formed upon cooling from the melt with liquid nitrogen and crystallizes within one week upon standing at room temperature. However, incorporation of twisted  $\pi$ -conjugated functional groups around the central core increases the possible number of conformations that the molecules can adopt resulting in more stable glasses with higher  $T_g$  (compounds **4-11**).

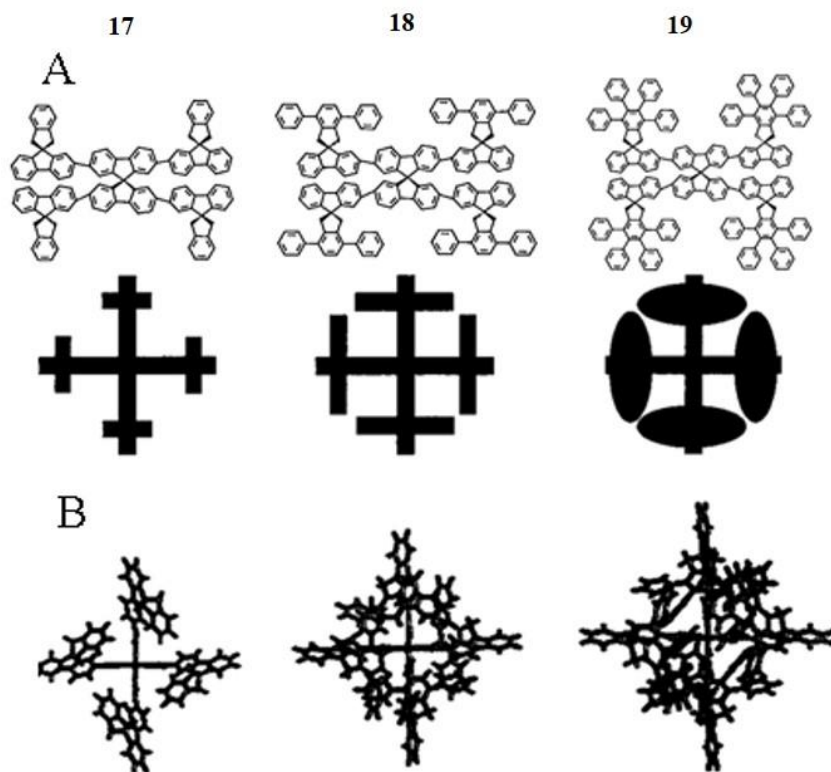


Figure 1: A) Fully spiro-configured terfluorene compounds and related molecular design concept. B) molecular structure taken from molecular calculations using the Amber software.

Nonetheless, replacing simple central cores with large groups would increase the size, volume and steric demand of the compound in order to prevent close packing and crystallization. As shown in series **12-14**, bulky central cores influence the conformation and subsequently affect the corresponding  $T_g$ . Although changing the core modifies the  $T_g$ , the main factor affecting glass formation is the nature and length of substituents around the core influencing the configuration. In compounds **12-14** with a tetrahedral geometry, the longer the conjugated fragments around the central core, the more stable the obtained glass, and the higher the  $T_g$ . In addition, the geometry of the arms around the central core minimizes cohesion between molecules and improves glass formation.<sup>17</sup>

Spirocyclic fluorene derivatives **15-19** form very stable glasses with the highest  $T_g$  among the compounds discussed above (above 200 °C). In this approach, the incorporation of sterically demanding and rigid spirocyclic groups in the core is stressed resulting in more stable glasses with high  $T_g$ , while in the glasses synthesized in the Shirota group, introduction of rigid groups around the center is emphasized. By integrating several  $\pi$ -conjugated substituents and spiro-shaped structures, glass-forming ability and stability are increased. In general the formation of glassy phases in all categories is based on the concept that introduction of rigid moieties within the structures increases  $T_g$  and higher molecular size enhances the stability of the amorphous state regardless of compound geometry.<sup>11</sup>

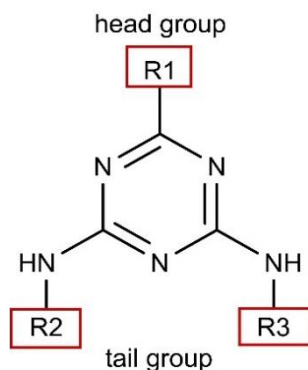
Among all compounds discussed so far, spiro derivative **19** exhibited the highest  $T_g$  (296 °C) due to its large molecular weight, bulky center, globular molecular shape and the configuration of aromatic rings which minimize non-covalent interactions. In general, more complex structures tend to show higher  $T_g$  and stability at ambient temperature, though at the cost of a more complex and costly synthetic procedure (table 1).

Table 1: Temperatures of glass-transition ( $T_g$ ), crystallization ( $T_c$ ), and melting ( $T_m$ ) for star-shaped compounds **1-19**.

<b>Compound</b>	<b><math>T_g</math> °C</b>	<b><math>T_c</math> °C</b>	<b><math>T_m</math> °C</b>	<b>Compound</b>	<b><math>T_g</math> °C</b>	<b><math>T_c</math> °C</b>	<b><math>T_m</math> °C</b>
<b>1</b>	8	60	90	<b>11</b>	183	261	298
<b>2</b>	50		162	<b>12</b>	190	-	246
<b>3</b>	35	103	171	<b>13</b>	165	-	-
<b>4</b>	76	117	260	<b>14</b>	191	-	-
<b>5</b>	132	168	-	<b>15</b>	112	-	-
<b>6</b>	109	154	279	<b>16</b>	170	-	427
<b>7</b>	121	196	269	<b>17</b>	225	-	-
<b>8</b>	63	-	-	<b>18</b>	275	328	452
<b>9</b>	127	174	264	<b>19</b>	296	-	-
<b>10</b>	163	-	-				

### 1.1.1.2.2. Mexylamine Triazine Based Molecular Glasses

The Lebel group has developed mexylaminotriazine derivatives as an outstanding family of long-lived glass forming compounds that are capable of forming supramolecular aggregates through non-covalent interactions such as hydrogen bonding and  $\pi$ - $\pi$  stacking intermolecular interactions.<sup>20</sup> The mexylaminotriazine motif contributes to frustrate crystallization in several ways: 1) by preventing close packing with the 3,5-disubstituted aryl groups, 2) by limiting molecular mobility with hydrogen bonding, and 3) by adopting several conformations of similar energy and with high interconversion barriers. In several libraries of these glasses, the impact of various structural elements at different positions of the diaminotriazine skeleton on glass forming ability and stability of the glassy phase have been investigated.



Scheme 1: Triazine glass with two tail groups and one head group.

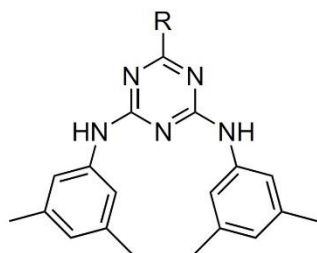
#### 1.1.1.2.2.1. The Influence of the Head Group

While it has been shown that both amino tail groups (which can be alkylamino or arylamino groups) are essential for the compounds to be capable of glass formation,<sup>21</sup> the functional group on the 2-position of the triazine ring (also called head group) has the most pronounced effect on the compounds' thermal properties

(Scheme 1).<sup>22</sup> Head groups can participate in hydrogen bonding, conjugation with the triazine ring and tautomerism which will affect the rotation, symmetry, planarity and size of the glass and subsequently the thermal properties of the compound.

A library of compounds possessing a bis-(mexylamino) triazine motif as the general structure and bearing different functional groups at the head group with alkyl chains of various lengths (presented as “R1” in scheme 1) was first studied.<sup>22</sup> The thermal properties of the compounds were measured by differential scanning calorimetry (DSC) and it was shown that most of the synthesized compounds were capable of glass formation with appreciable resistance to crystallization. A wide range of functional groups could be thusly introduced, and most compounds proved capable of forming glassy phases with  $T_g$  ranging from 26-97 °C.<sup>23</sup>

Only a few head-groups studied did not promote glass formation: unsubstituted, chloro, hydroxyl, thiol, carboxylic acid, carboxamide, and mexylamino (**20-26**). The structure and interaction of head group in such compounds are in a way that facilitate close packing and crystallization, owing to either higher symmetry (NH mexyl), strong hydrogen bonding (CO<sub>2</sub>H, CONH<sub>2</sub>, OH, SH), tautomerism (OH, SH), or small size (H, Cl).



- 20:** R= OH
- 21:** R= SH
- 22:** R= CONH<sub>2</sub>
- 23:** R= NHMexyl
- 24:** R= H
- 25:** R= Cl
- 26:** CO<sub>2</sub>H

In this study, it is shown how the introduction of structural elements within the skeleton of the molecule can exploit self-association between the molecules along specific patterns by influencing intermolecular non-covalent interactions. In this study, directional interactions and conformations that usually promote crystallization in small and relatively rigid molecules, has been shown to work against it.<sup>12</sup> Unlike traditional guidelines that rely on nonplanarity as a major cause for glass formation ability, these compounds can adopt a planar geometry. Molecular structure in such compounds is designed in a way that supports amorphous phase formation, and non-covalent interactions, especially hydrogen bonds between bis(mexylamino)triazine groups and the head groups, contribute to

frustrate crystallization by promoting the formation of aggregates that pack poorly, and by limiting the reorganization of molecules to the crystalline state.<sup>12</sup>

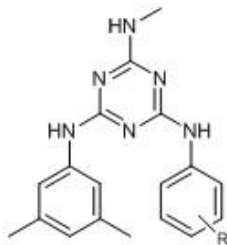
The other important parameter to influence the thermal behavior of the compounds is the length of the alkyl chain at the head group. The compounds bearing alkyl chains that are either too short or too long show poor glass-forming ability and eventually crystallize upon slow heating. However, the ideal size of the alkyl chain depends also on the nature of the functional group. For instance, ester-substituted derivatives bearing hexyl or longer alkyl chains show poor glass forming ability and crystallize upon heating under the melting point while for the case of tertiary amines with linear alkyl chains smaller than butyl, crystallization readily occurs upon heating.<sup>23</sup> While increasing the alkyl chain length causes  $T_g$  to decrease, branched alkyl chains tend to show higher  $T_g$  values than linear chains of the same size.<sup>23</sup>

In these cases, solid state packing is facilitated by alkyl chains of non-optimal size which results in crystallization. Alkyl groups interactions are limited to London forces, but when alkyl chains reach a certain length, the interactions become strong enough to allow reorganization of the molecules in an ordered fashion, thereby leading to crystallization. Furthermore, as longer alkyl chains lower  $T_g$  because of their flexibility, molecular mobility at ambient temperature is enhanced.

#### 1.1.1.2.2. The Influence of the Tail Groups

The nature and length of the functional groups on the 4- and 6-positions of triazine ring (also called tail groups or ancillary groups) can also influence the polarity, symmetry, non-covalent interactions and molecular weight of the molecule which subsequently have an impact on the thermal properties of the glasses.

In one study, a library of derivatives was synthesized with one tail group being functionalized with various arylamino or cycloalkylamino substituents.<sup>21</sup> The head group and the other tail group were kept constant as methylamino and mexylamino groups, respectively (Scheme 2).



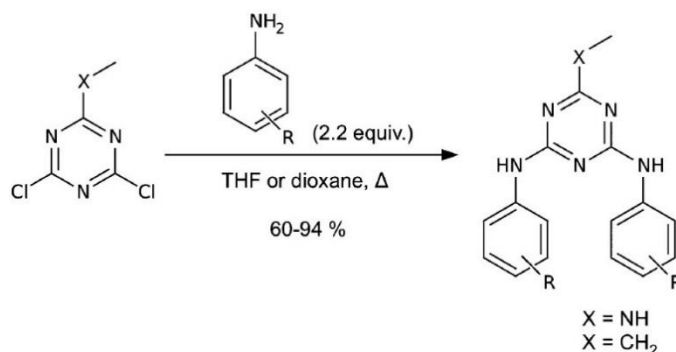
Scheme 2: Mexylaminotriazine glass.

The synthesis was performed by sequential substitution on cyanuric chloride with the respective amines. The impact of various substituents on glass-forming ability and on  $T_g$  was examined. It was shown that replacing one of the mexylamino groups with other arylamino or alkylamino groups does not inhibit the formation of glassy phases and all mexylaminotriazine derivatives studied were able to form amorphous phases. The range of measured  $T_g$  was between 52-131 °C and only one of the derivatives (2,4,6-trimethylphenyl-substituted) recrystallized upon heating at a rate of 5 °C/min. It was also observed that substituted aryl functional groups typically show  $T_g$  in the order *ortho* < *meta* < *para*. One possible explanation is that *para*-substituted compounds exhibit higher symmetry while *ortho* substituents obstruct hydrogen bonding. In general, substituents that are able to participate in hydrogen bonding such as OH, NH<sub>2</sub>, CONH<sub>2</sub>, CO<sub>2</sub>H, tend to show higher  $T_g$  values.

After confirming that one tail group could be substituted without loss of glass-forming ability, the impact of substituting both mexylamino tail groups on glass-forming ability and stability were investigated in a separate study.<sup>22</sup> Two series of compounds were synthesized, one bearing a methylamino head group which is known to promote extremely stable glassy phases,<sup>21</sup> and the other series with an ethyl head group with mediocre glass-forming ability. Both tail groups were kept identical for each member of both series. Once again, the synthesis of derivatives involved the reaction of a 4,6-dichloro-1,3,5-triazine precursor with the corresponding amines (Scheme 3). Surprisingly, almost all the compounds with a NHMe head group possessed the ability to form amorphous phases with a  $T_g$  in the range of 22 to 129 °C, while for the series with an ethyl head group, only 15 compounds out of 21 showed any capacity to form glasses with glass transition temperatures between 19 and 96 °C. It was also determined that most compounds with a NHMe head group capable of amorphous phase formation showed high glass stability. However, for the case of compounds bearing an ethyl head group, much lower glass stability was observed for the few compounds capable of amorphous phase formation; in most cases crystallization occurred within 1-3 days on standing. Interestingly, the bis(mexyl) derivative was the compound of the ethyl series with the best glass-forming ability and glass stability. These observations are due to the structure of the NHMe head group that is both 1) capable of participating in hydrogen bonding, and 2) strongly conjugated with the triazine ring, thereby limiting molecular motion in the solid and resulting in higher glass stability compared to their ethyl (Et) analogues. In addition to the influence of the nature of tail groups on thermal properties, the impact of tail group symmetry was studied.<sup>22</sup> Very similar thermal behavior was observed between compounds with identical tail groups and their analogues with different tail groups) and it was shown that the

increased molecular symmetry generated by bearing two identical tail groups does not impact significantly the thermal properties of candidates.

In this study, the impact of various aryl and alkyl tail groups on the thermal properties of the diaminotriazine scaffold was investigated and it was shown that aryl groups are capable of formation of glassy phases with a high  $T_g$  due to the rigidity of the aryl moieties. However, alkyl ancillary groups show poor glass forming ability with low  $T_g$  compared to arylamino-substituted compounds. Actually, for compounds with alkyl ancillary groups, only compounds with a methylamino head group formed glassy phases. Arguably, the  $\pi$ - $\pi$  interactions in aryl-substituted compounds contributes to establish a disordered network which prevents the close packing of molecules and promotes glass formation.



Scheme 3: Synthesis of mexylaminotriazine glasses.

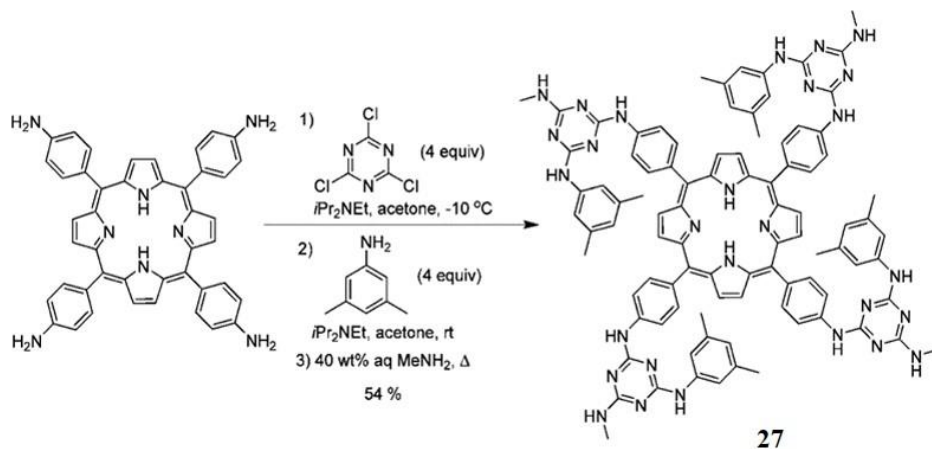
In both star-shaped and mexylaminotriazine molecular glasses,  $\pi$ - $\pi$  interactions are present, but in both cases, the aromatic surfaces are not very large (aromatic rings are twisted out of planarity in star-shaped compounds), and aromatic rings can interact along several different orientations. The fact that  $\pi$ - $\pi$  interactions in these systems are non-directional and non specific contributes to prevent the formation of ordered networks.<sup>23</sup>

#### 1.1.1.2.2.3. Mexylaminotriazine Functionalized Dyes

Functional groups located on aryl substituents on mexylaminotriazine glasses are capable of reacting with other compounds which are incapable of amorphous phase formation by themselves such as dyes, semiconductors, fluorophores, ligands for transition metals, and calixarene derivatives.<sup>24</sup> In the following examples, inducing glass formation in tetraphenylporphyrin (TPP)<sup>25</sup> and Disperse Red 1 (DR1)<sup>26</sup> through functionalization with mexylaminotriazine glasses will be described.

Mexylaminotriazine units were built on a tetraphenylporphyrin (TPP) core by successively reacting tetrakis(4-aminophenyl)porphyrin with cyanuric chloride, 3,5-dimethylaniline and methylamine in a one-pot procedure, giving adduct **27** in 54% yield (Scheme 4). The  $T_g$  measured with DSC was 205 °C and further heating above  $T_g$  did not cause crystallization, in contrast to the parent TPP that readily crystallizes and melts at 444 °C.

As demonstrated in the previous study, mexylaminotriazine units are capable of attaching to another core such as a dye and impart glass forming ability on the linked moiety. However, the synthetic procedure, while one-pot, gave mediocre yields and many side products that had to be separated by chromatography. Furthermore, only one mexylaminotriazine group is necessary to induce glass formation, the other three present in compound **27** only needlessly increase its molecular weight while decreasing its solubility in most organic solvents. The synthetic strategy could thus be improved by reacting the dye with a glass holding a reactive functionalizable group in a straightforward, one-step procedure. Various mexylaminotriazine glasses have been synthesized containing reactive groups capable of attaching to other compounds via covalent bonds, some examples are presented (compounds **28** to **30**).<sup>21</sup>



Scheme 4: Synthesis of molecular glass **27**.

In order to design novel azobenzene glasses, glass **28** bearing an alkylamino functional group was selected to react with Disperse Red 1 (DR1) via a carbamoylation reaction (Scheme 5). In this method, the hydroxy group on DR1 is functionalized in a simple way under mild conditions. The innovative azobenzene glass was synthesized by first reacting DR1 with *N,N*-carbonyldiimidazole (CDI). The resulting intermediate was then reacted with glass precursor **28** to obtain the



organic light-emitting diodes (OLEDs), organic photovoltaic devices (OPVs), organic field-effect transistors (OFETs) and photochromic devices.<sup>29</sup>

### **1.2.1. Pharmaceutical Glasses**

Amorphous pharmaceutical products are important due to two main factors.<sup>27</sup> Firstly, amorphous solids enjoy greater solubility, enhanced dissolution and better compressibility characteristics compared to the corresponding crystals.<sup>27</sup> Second is that because of the instability of amorphous solids, molecules tend to be less stable in the glassy phase than in the crystalline phase both physically and chemically. It is therefore important to prevent the degradation, both of the molecules themselves and of the glassy phase.<sup>28</sup>

Some drugs can exist naturally in the amorphous phase.<sup>27</sup> In some cases, however, the amorphous state may be introduced deliberately to the drug, excipient or delivery system to improve the performance and biopharmaceutical properties of the product.<sup>27</sup> For many medications, the rate-limiting step to absorption is the dissolution in the gastrointestinal system, therefore preparing the drug in its amorphous form increases the molecular mobility and leads to enhanced dissolution rate and bioavailability.<sup>28</sup>

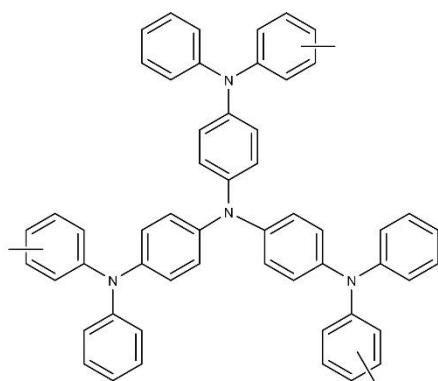
### **1.2.2. Electronic and Optoelectronic Applications**

Amorphous organic semiconductors, also known as amorphous organic charge transport materials, can be used in electronic and optoelectronic devices such as organic light emitting diodes (OLEDs), organic photovoltaic cells (OPVs) and organic field-effect transistors (OFETs).<sup>29</sup> The charge transporting materials are classified into three groups of *p*-type (hole-transporting), *n*-type (electron transporting), or bipolar (electron and hole transporting).<sup>11</sup>

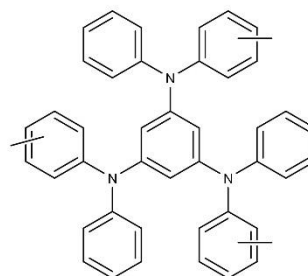
Hole-transporting materials are materials that accept hole carriers and transport them, possessing low ionization potential with low electron affinities. On the other hand, materials with high electron affinities and high ionization potentials function as electron transporting materials and transport electron carriers.<sup>11</sup> The materials capable of transporting both holes and electrons are called ambipolar. From the point of view of charge transport mechanism, the transport of electrons and holes takes place by a hopping process. That is a sequential redox process through the lowest unoccupied molecular orbital (LUMO) and highest occupied molecular orbital (HOMO) over the molecules.<sup>29</sup>

### 1.2.2.1. Organic Light Emitting Diodes (OLEDs)

In OLED devices, organic semiconductors are located between two electrodes as an emissive electroluminescent layer that emits light in response to an electric current.<sup>2</sup> Charge injection from the electrodes into the organic layers followed by the transport of charge carriers through the organic layers results in the formation of excitons (electronically excited states of molecules) that are generated by the combination of holes and electrons.<sup>2</sup> Deactivation of excitons occurs by emission of light by fluorescence and phosphorescence (electroluminescence).<sup>2</sup> The operation of OLEDs depends on the materials used in the different parts of the device such as charge injection layer, charge transporting layer, charge blocking layer and emission layer.<sup>29</sup> Requirements for materials used in OLEDs are as follows: 1) they should be capable of forming uniform thin films without pinholes 2) the materials should be thermally and morphologically stable, and 3) they should have high electron affinity and ionization potential to be able to inject the charge carriers in to the layers next to them.<sup>29</sup>



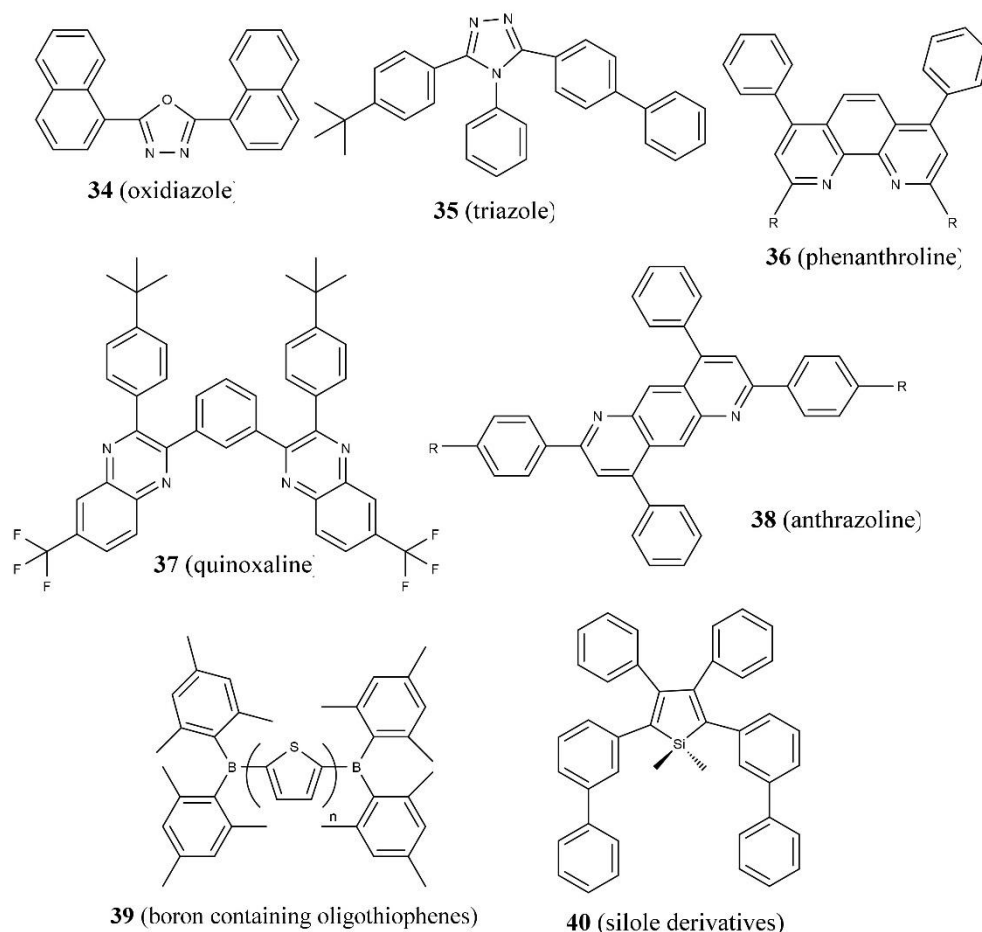
32 (TDATA family)



33 (TDAB family)

Molecular glasses have been proven to be perfect candidates for OLEDs. Depending on the hole or electron drift mobility, glasses can transport charge carriers through them.<sup>2</sup> Numerous star-shaped families of hole transporting amorphous materials in OLEDs have been developed including compounds having triphenylamine **32** (TDATA),<sup>30</sup> **33** (TDAB),<sup>31</sup> and tetraphenylmethane and spirobifluorene (**17-19**) as central core.

Similar to hole transporting amorphous molecular materials, the electron transport layer should have high drift mobility to be capable of functioning as a transporting layer in OLEDs. Some of these compounds play a role in hole-blocking as well as electron acceptance and transport. The electron transporting amorphous molecular materials should be designed to include electron-withdrawing moieties within their structure.<sup>29</sup> Based on the central structural units, electron transporting materials can possess various geometries among the following: compounds with triazine, triphenyltriazine, benzene, triphenylbenzene, tetraphenylsilane and tetraphenylmethane, 1,3,4-oxadiazole (**34**),<sup>32</sup> triazole (**35**),<sup>33</sup> phenanthroline (**36**),<sup>34,35</sup> quinoxaline (**37**),<sup>36</sup> anthrazoline (**38**),<sup>39</sup> boron-containing oligothiophenes (**39**),<sup>37</sup> and silole derivatives (**40**).<sup>38</sup>



### 1.2.2.2. Organic Photovoltaic Devices (OPVs)

OPVs are devices that transform light energy into electrical energy which have attracted the attention of researchers in the past few decades because of their low cost, light weight, large area and flexible device fabrication.<sup>39</sup> The operation involves absorption of light by the organic layer followed by production of an exciton. The exciton diffuses and generates charge carriers by electron transfer, resulting in the collection of charges at the electrodes.<sup>2</sup> There are mainly two device structures, one is called Schottky type and is based on a single organic layer sandwiched between two different electrodes. The other is a *pn*-heterojunction structure in which a double-layer (*p*-type and *n*-type) organic thin film is sandwiched between two electrodes and the interaction of electron acceptor and electron donor groups at the interface of two semiconducting layers plays an important role in the generation of charge carriers.<sup>11</sup>

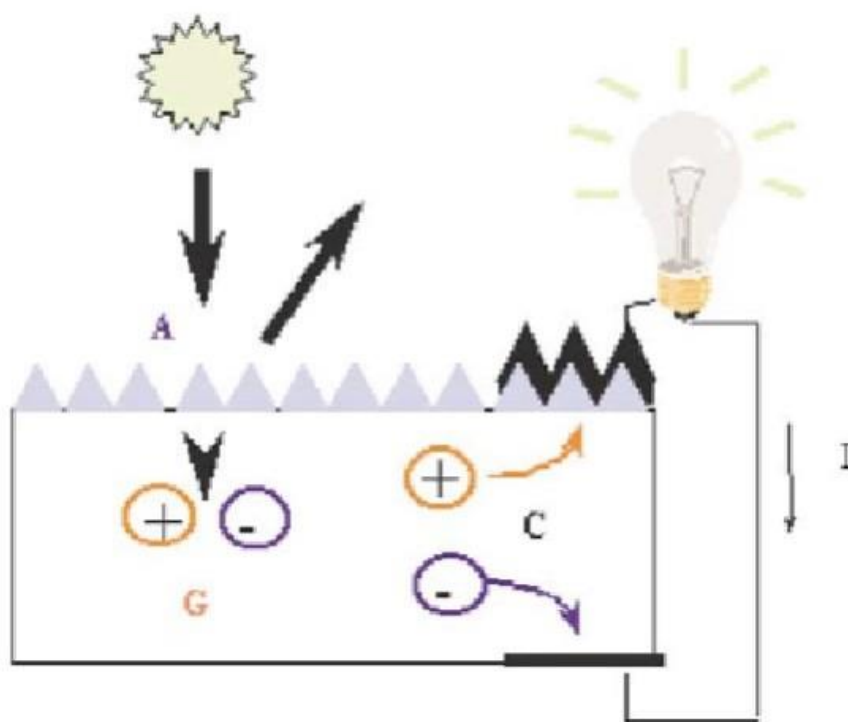
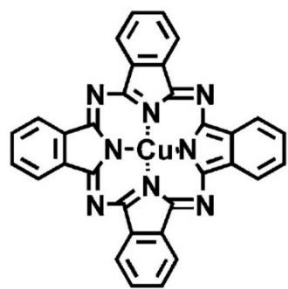


Figure 2: The photovoltaic process: absorption of photons (A) generation of carriers (G), collection of carriers (C).<sup>39</sup>

In both Schottky-type and *p-n* heterojunction cells, low molecular weight molecules have been used. Small molecules such as copper phthalocyanine CuPc (**41**) and C<sub>60</sub> (**42**)<sup>41, 42</sup> tetracene (**43**)<sup>43</sup> and pentacene (**44**)<sup>44</sup> have been used as semiconductors. However, compounds **41-44** are not capable of forming glassy phases.

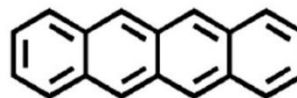
Molecular glass *m*-TDATA (**32**) has been reported as an organic layer between indium tin oxide (ITO) and aluminum electrodes in Schottky type devices.<sup>30</sup> Compound **32** has been also used as an electron donor and and tris(8-hydroxyquinolino)aluminium (Alq<sub>3</sub>) **45** as electron acceptor in double layer cells.<sup>40</sup>



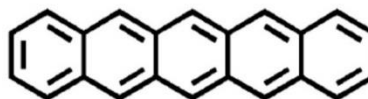
**41** (CuPc)



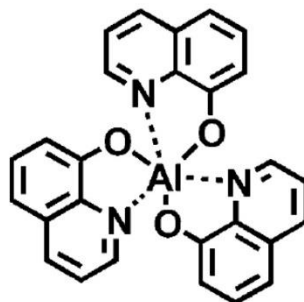
**42** (C<sub>60</sub>)



**43** (tetracene)



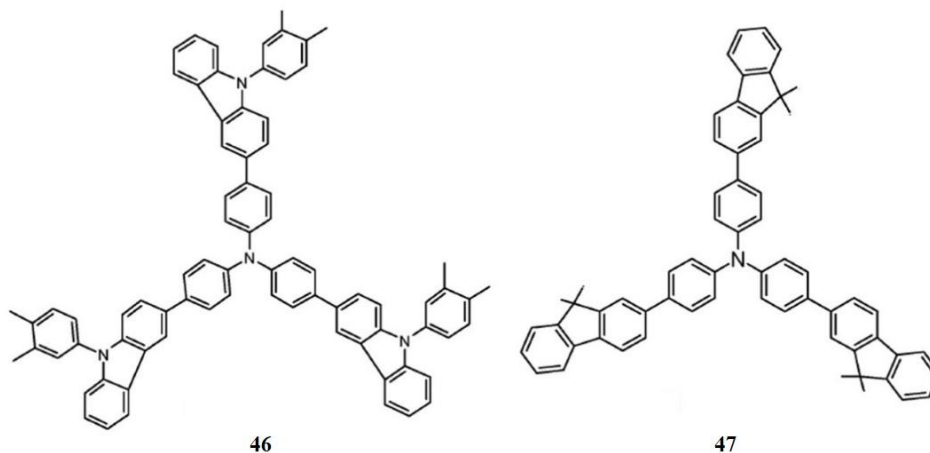
**44** (pentacene)



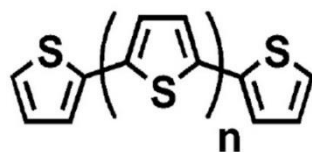
**45** (Alq<sub>3</sub>)

### 1.2.2.3. Organic Field Effective Transistors (OFETs)

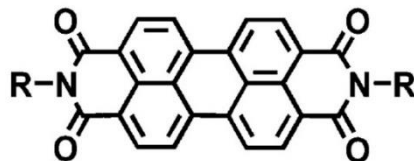
OFETs are charge carrier devices which consist of three electrodes (source, drain and gate), an insulator and an organic semiconductor layer. By applying a potential to the gate electrode, a depletion layer will be formed in the semiconductor layer (channel) which increases the conductivity of the channel between the drain and the source. This state is called on-state of transistor, where the electrons and holes can be injected from the source electrode into the organic semiconductors and transported toward the drain electrode. The conductivity of channels is dependent on the potential applied on the gate. When the device is at rest, no potential is applied on the gate, the transistor is in the off-state and thus there will be no injection of electrons and holes from the source electrode through the semiconductor layer.<sup>29</sup> There is an insulator between the gate electrode and the semiconducting layer to isolate the charges on the gate electrode. This will polarize the gate electrode and the semiconductor layer to induce a depletion layer in the semiconducting layer.<sup>29</sup> The semiconducting layer can be electron-donating or electron-accepting, forming *p*- or *n*-channels respectively.



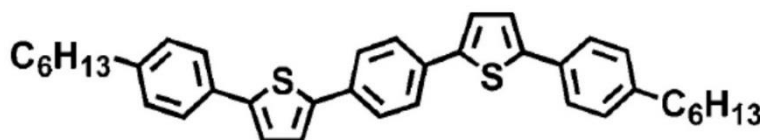
Most organic compounds used in OFETs are used in the crystalline state, including oligothiophenes and their analogues (**48**),<sup>45</sup> phenylene-thienylene oligomers (**49**),<sup>46</sup> tetracene or pentacene (**43**, **44**),<sup>72</sup> perylenediimide dyes (**50**),<sup>48</sup> and fullerenes. (**42**).<sup>49</sup> However, promising results were also reported using compounds that are capable of forming stable glassy phases, such as triphenylamine-based compounds with carbazole or fluorene side arms (**46**, **47**).<sup>50</sup>



48 (oligothiophenes)



50 (perylene-3,4,9,10-tetracarboxylic diimide dye)



49 (phenylene-thienylene)

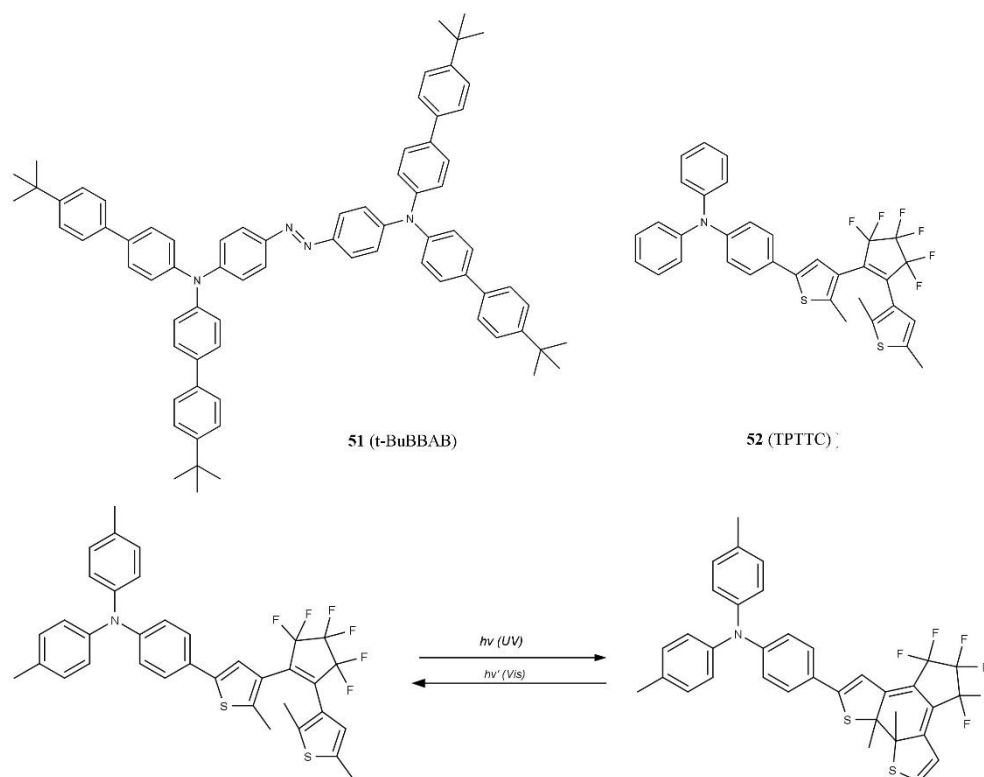
### 1.2.3. Photochromic Amorphous Molecular Materials

Photochromism is defined as the reversible transformation of a chemical species by absorption of electromagnetic radiation between two forms, each having a different absorption spectra.<sup>51</sup> The potential applications of photochromic materials are image formation, optical data storage and optical switching.<sup>2</sup> In order to use such materials for the aforementioned applications, they need to be used in the form of a solid film. For this purpose, polymeric photochromic chromophores and photochromic compounds dispersed in polymer binders have been the focus of research.<sup>11</sup> However, an alternative option to polymeric chromophores consists in using amorphous molecular materials possessing photochromic groups that are capable of uniform thin film formation.

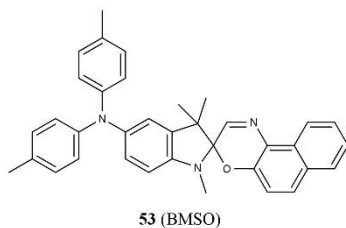
Photochromic molecular glasses previously reported include compounds with azobenzene chromophores such as 4,4'-bis[bis(4'-tert-butylbiphenyl-4-yl)amino]azobenzene (t-BuBBAB) **51**. Irradiation of this compound with 450 and 550 nm light causes the photoisomerization of the azobenzene group from *cis*- to *trans*- and vice versa repeatedly.<sup>11</sup> More than 80% of the compound in the *cis*-form stays unchanged at room temperature after five days, although the *cis*-form isomerizes to the *trans*-form completely by heating at 140 °C.

In addition to the azobenzene family, dithienylethene-based compounds have been studied extensively in solution. Typically, irradiation of dithienylethene derivatives with UV light (360-580 nm) triggers a ring closure reaction which converts the colorless open form into the colored closed form (photocyclized form). The reverse reaction (ring opening) to regenerate the open form takes place on irradiation with visible light with wavelengths higher than 580 nm (Scheme 6).<sup>52</sup> The addition of diarylamino moieties on the dithienylethene core results in

chromophores that are capable of forming amorphous glasses with well-defined  $T_g$ .<sup>11</sup> One example of dithienylethene-based compounds include 1-{5-[4-(di-p-tolylamino)phenyl]-2-methylthiophen-3-yl}-2-(2,5-dimethylthiophen-3-yl)-3,3,4,4,5,5-hexafluorocyclopentene (TPTTC) **52**. These compounds exhibited similar photochromic properties both in solution and as amorphous films.<sup>52</sup>

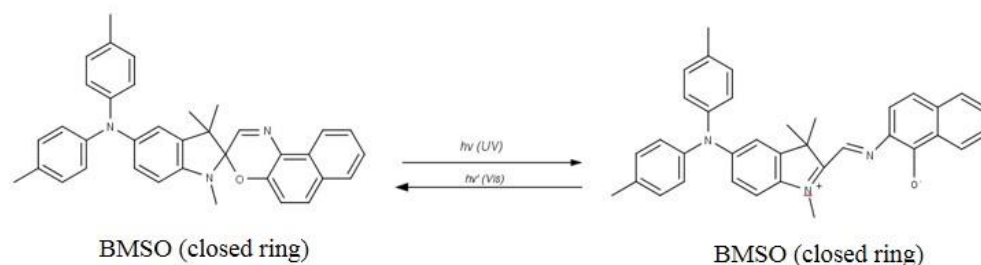


Scheme 6: Ring closure-ring opening reaction of TPTTC upon irradiation with UV-light.



Other examples of photochromic amorphous molecular materials include spirooxazine- based materials such as 5-[bis(4-methyl-phenyl)amino]-1,2,3-trimethylspiro{indoline-2,3'- (3H-naphth[2,1-b][1,4]oxazine)} (BMSO) **53**.<sup>53</sup> Upon

irradiation of BMSO with 365 nm-light, a ring-opening reaction takes place to generate the colored merocyanine form (Scheme 7). Reverse cyclization occurs by irradiation with visible light (>580 nm).



Scheme 7: Ring closure-ring opening reaction of BMSO upon irradiation with UV-Vis light.

#### 1.2.4. Nanolithography Applica

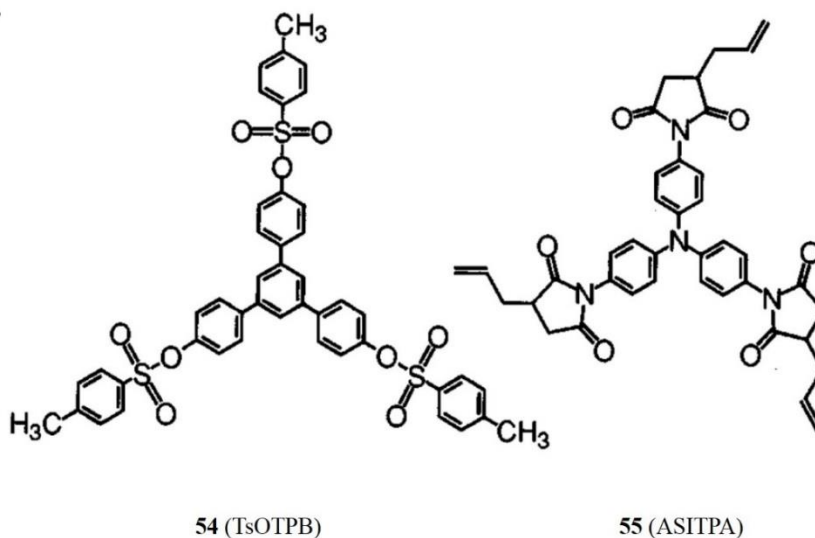
Nanolithography refers to lithographic patterning methods used to generate features smaller than 100 nm. Lithography is a method of printing by formation of three-dimensional images on a substrate by subsequent transfer of patterns to a substrate. In semiconductor lithography, the patterns are written with a light-sensitive polymer, where a photochemical reaction results in the cross-linking of the polymer chains exposed to light.<sup>54</sup> A mask is used to shield selected parts of the substrate from the light treatment.

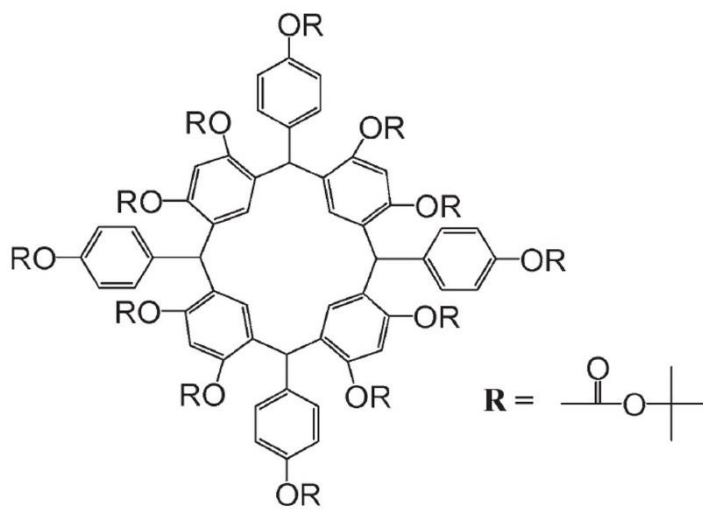
Low molecular weight compounds are considered promising alternative choices compared to polymers in the field of nanolithography. Molecular glasses that do not crystallize on the time scale of use and that allow the formation of uniform and transparent thin films with isotropic properties can be used to generate patterns that are smoother and higher-quality relative to larger polymers.<sup>55</sup> Low line edge roughness is considered as the main advantage of molecular glasses compared to polymers. Line edge roughness (LER) is defined as a deviation from fitted line of the edge of a feature, averaged across several features. The small size of low molecular weight resists results in higher resolution features through smaller pixel sizes.<sup>56</sup>

The other significant difference between polymeric resists and molecular glass resists is polydispersity. Polymers consist of a range of molecular weights while molecular glasses are monodisperse. Therefore the dissolution rate is

comparatively constant across the exposed region in a homogeneous manner which leads to less residual stress swelling and minimum chain entanglements. Although for the case of polymers, polymers with low molecular weight have higher dissolution rate compared to high molecular weight polymers. Therefore the dissolution behavior of a polymeric base resist is a composite value which depends on its molecular weight distribution.<sup>56</sup>

Novel low molecular-weight organic materials synthesized for nanolithography are expected from glasses, a few examples being 1,3,5-tris[4-(4-toluenesulfonyloxy)phenyl]benzene (TsOTPB) **54**,<sup>55</sup> 4,4',4''-tris(allylsuccinimido)triphenylamine (ASITPA) **55**<sup>55</sup> and C-4-hydroxyphenyl-calix-[4]resorcinarene **56**.<sup>56</sup> Their lithographic properties were evaluated and it was shown that ASITPA and TsOTPB resists have high resolution capability and are able to generate line patterns smaller than 150 nm. Both ASITPA and compound **56** can undergo a polymerization reaction triggered by the presence of catalytic amounts of a photoacid generator (PAG), typically a triphenylsulfonium salt. This reaction generates a cross-linked polymer in irradiated areas. Compound **56** was shown to be able to form amorphous phases and feature sizes as small as 30 nm with low LER.<sup>56</sup>





56 (C-4-hydroxyphenyl-calix-[4]resorcinarene)

### 1.3. Statement of Research Objectives

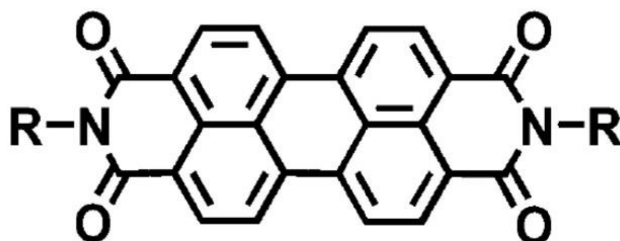
The focus of this thesis is twofold. The first being the synthesis and characterization of perylene diimide (PDI) and fullerene-functionalized molecular glasses by covalent bonding of these compounds to methylaminotriazine molecular glasses, and the second being the investigation of the thermal and optical properties of the synthesized solids by UV-Vis spectroscopy and differential scanning calorimetry (DSC). Chapter 2 discusses the synthesis of PDI dyes functionalized with molecular glass **29**, and the investigation of glass formation by the products. Chapter 3 focuses on the synthesis and characterization of methylaminotriazine-functionalized fullerene derivatives. In Chapter 4 this dissertation will be summarized and future perspectives for further developments of the project will be described.

## 2 PDI-Functionalized Molecular Glasses

### 2.1. Introduction

#### 2.1.1. Definition and Properties of PDI Dyes

Perylenediimides (PDIs) are a family of polycyclic aromatic compounds which show a very strong absorption in the visible region.<sup>57</sup> Derivatization of perylenediimide dyes can be used to influence the structural and electronic properties of the ring system. In fact, a considerable amount of research on perylenediimide derivatives has been performed to either tune the absorption of the molecules to specific bands, increase the range of frequencies absorbed or tune their electron transport properties.<sup>58</sup> One of the most important characteristics of PDIs is the conjugated  $\pi$  system of the polycyclic aromatic structure which makes such compounds suitable candidates for optoelectronic applications. Unlike perylene itself, the four electron-withdrawing carbonyl groups on the PDI unit make the aromatic system electron-deficient, thereby making perylenediimide an electron acceptor. In addition to their electronic properties, PDI dyes possess a number of other desirable properties such as good weather stability, high thermal stability and good photo-stability.<sup>59</sup>



50 (perylenediimide dye)

#### 2.1.2. Applications

PDI compounds have a wide range of applications. The electronic properties of PDI-based compounds have made them appealing functional dyes for applications in molecular electronic devices such as thin film transistors, and as high performance *n*-type materials in photovoltaic cells, thin film transistors (TFTs) and organic light emitting diodes (OLEDs).<sup>60</sup> The optimal PDI derivative for each application can be obtained by proper engineering of the perylene core and

attaching different functional groups to alter their physical and chemical properties.<sup>61</sup> Functionalization with electron-donor or acceptor groups can drastically alter the optical and electronic properties of the chromophore. In addition to these applications, PDI-based materials are also used in laser electrophotography (xerographic photoreceptors) and fluorescent light collectors.<sup>62</sup>

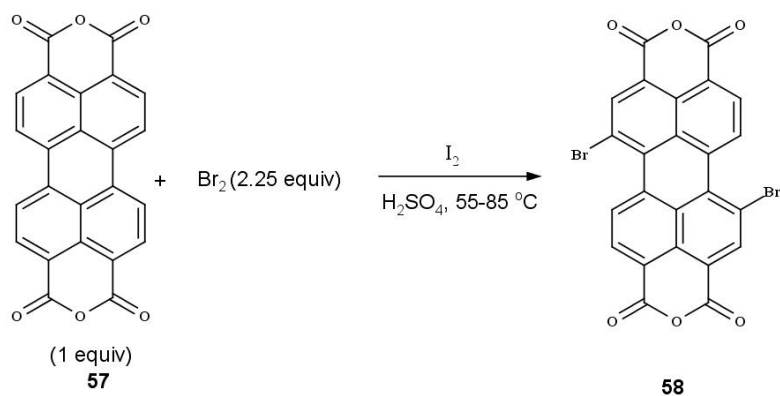
### **2.1.3. Potential Applications of PDI-Functionalized Molecular Glasses**

Functionalization of PDI derivatives with mexylaminotriazine molecular glasses is expected to induce glass-forming properties in the corresponding derivatives. Materials capable of amorphous phase formation have benefits over crystalline materials in device fabrication due to their transparency, good processability from solution, and homogeneous and isotropic properties. Perylenediimides are the most common acceptors studied in OPVs after fullerenes and have shown among the highest *n*-type mobilities reported so far.<sup>63</sup> Therefore, glass-forming derivatives of this family are considered to be potential high-performance *n*-type candidates to be utilized as amorphous charge-transporting materials in electronic and optoelectronic devices such as OLEDs and OPVs.<sup>63</sup>

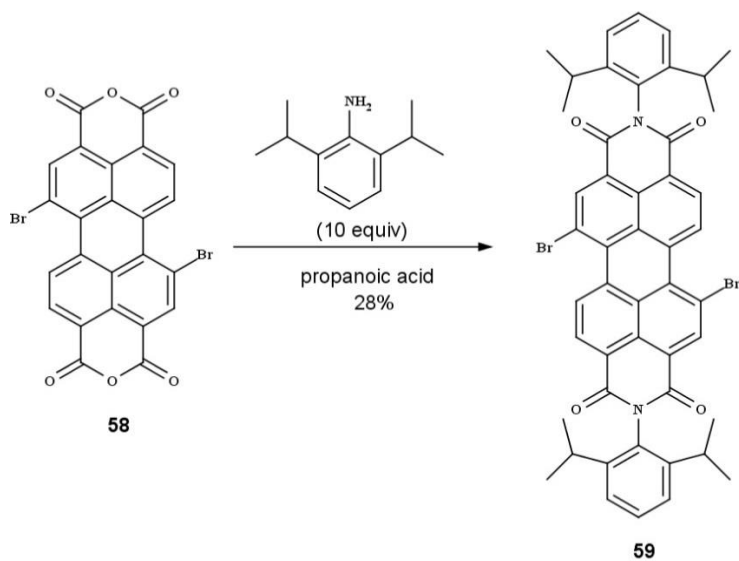
Compounds **60**, **61**, and **62** described in the following sections are PDI-functionalized molecular glasses, synthesized by the reaction of thiol-functionalized glass **29** with 1,7-dibromo PDI derivatives (Schemes 8-13). The synthesis, thermal, optical and electronic properties of candidates will also be reported in the following sections.

## **2.2. Results and Discussion**

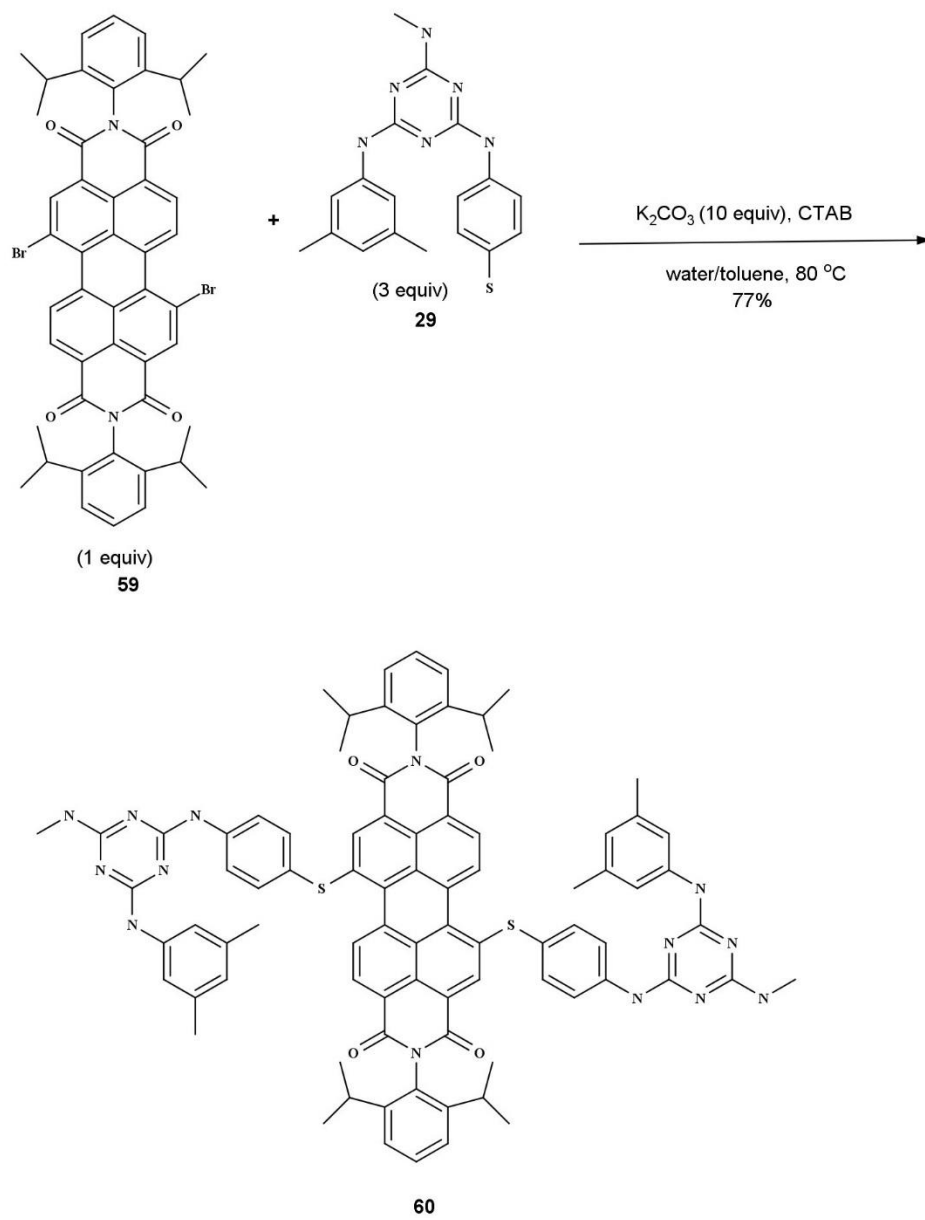
The synthesized PDI-functionalized molecular glasses and the corresponding synthetic routes are presented in Schemes 8-13.



Scheme 8: Synthesis of compound **58**.

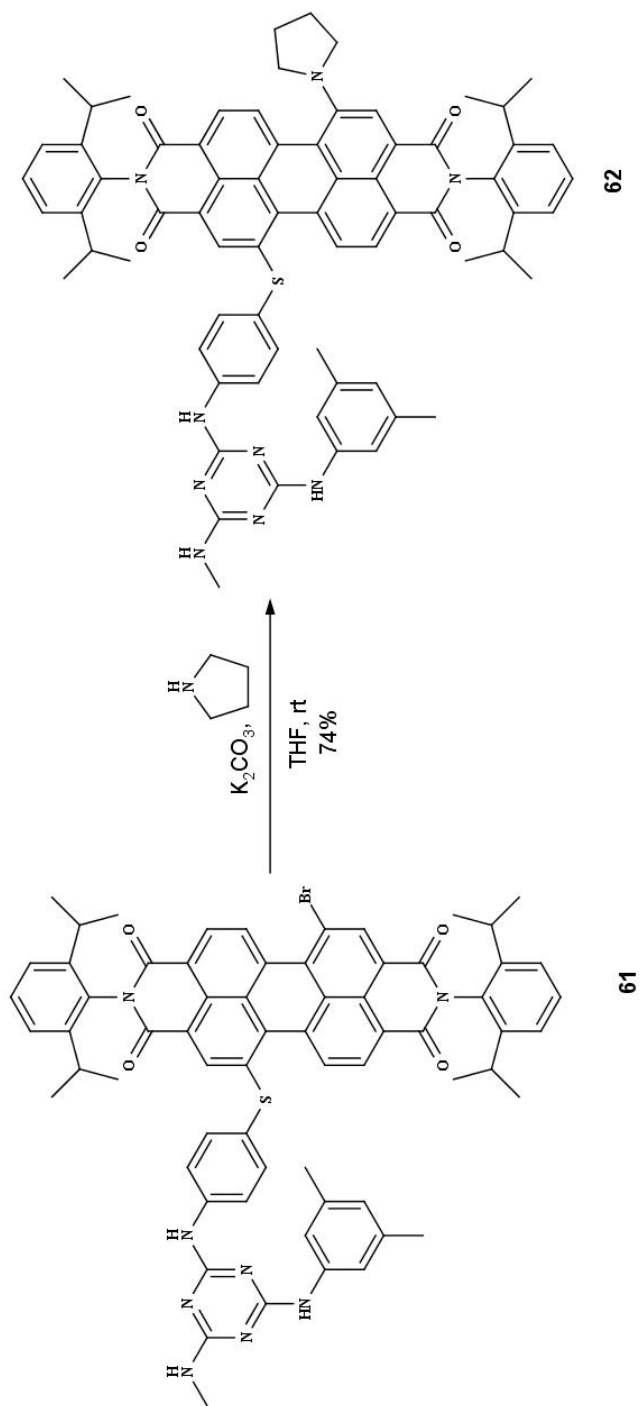


Scheme 9: Synthesis of compound **59**.

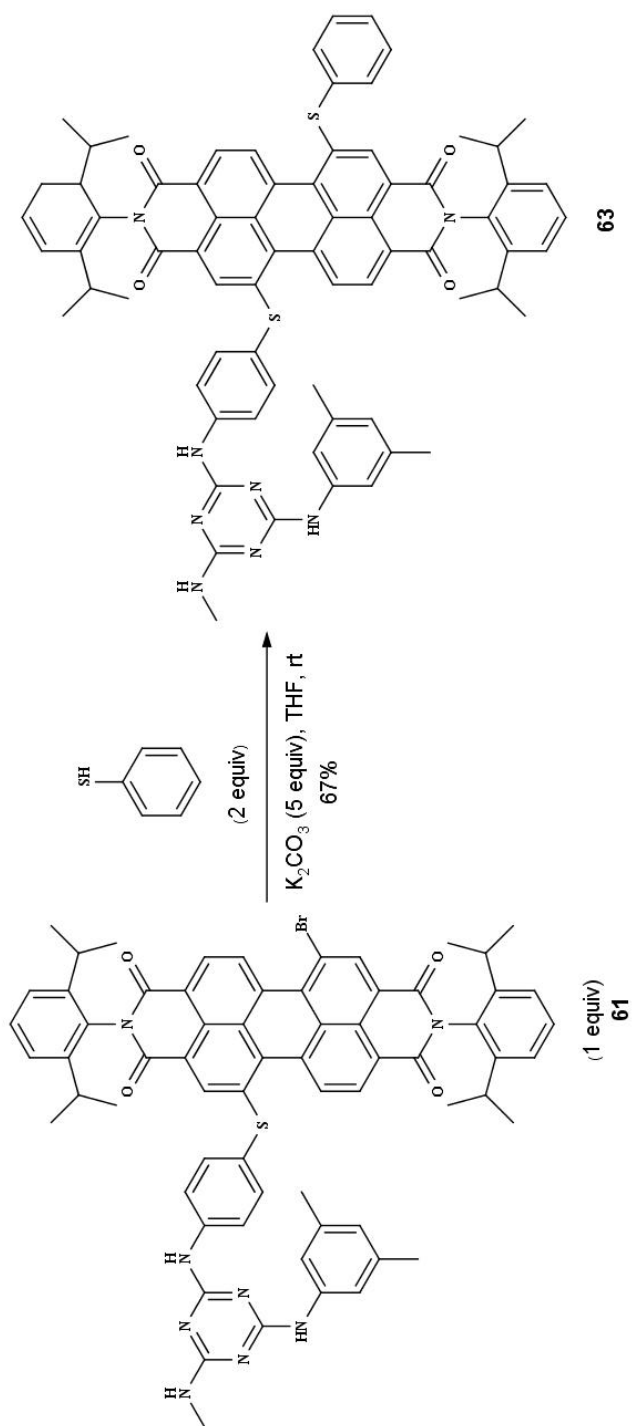


Scheme 10: Synthesis of compound **60**.





Scheme 12: Synthesis of compound **62**.



Scheme 13: Synthesis of compound **63**.

### 2.2.1. Synthesis and Characterization

Perylenetetracarboxylic bisanhydride was the common starting material to synthesize the candidates. Synthesis of precursor **58** was performed according to a literature procedure<sup>61</sup> involving the bromination of the bisanhydride through an aromatic electrophilic substitution reaction (Scheme 8). The crude product was taken directly to the next step because of its insolubility in organic solvents. In the following step, the imidization of compound **58** was performed by refluxing intermediate **58** with excess 2,6-diisopropylaniline in propionic acid to afford precursor **59** in 28 % global yield after purification. The introduction of diisopropylphenyl functional groups on the perylene ring improved its solubility in organic solvents and simplified the process of characterization. The <sup>1</sup>H NMR spectrum of diimide **59** shows peaks at 9.03 and 9.56 ppm, which correspond to bay region protons next to the bromo groups, while the peak at 1.05 ppm, which integrates to 24 protons, corresponds to methyl protons on the 2,6-diisopropylaniline groups.

Compound **60** was obtained from precursor **59** by a one-step nucleophilic substitution of the bromo groups with thiol glass **29**. Three equivalents of compound **29** were used to make sure that both bromo groups were substituted and 77% pure disubstituted PDI glass **60** was obtained. While the product readily precipitates out of the reaction mixture and be conveniently purified by washing with dichloromethane, which conveniently removes glass **29**, starting material **59** and monosubstituted product **61**, the product is nonetheless soluble in polar organic solvents such as THF, DMF or DMSO and therefore the product could be easily characterized by NMR spectroscopy. In the <sup>1</sup>H NMR spectrum of compound **60** the peak at 9.56 ppm from the protons in the bay region was replaced by a peak at 8.29 ppm, confirming that both bromo groups were replaced by glass moieties. The other peaks corresponding to the aromatic protons on the bay region were also shifted relative to precursor **59**, and each signal integrated for 2 protons, as a consequence of symmetry. In addition, the disappearance of the SH proton and shifting in the chemical shift of protons *ortho* to the thiol group proves the attachment of the methylaminotriazine units to the PDI core.

The monosubstituted, monobromo analogue **61** was synthesized by a nucleophilic substitution of dibromoperylene diimide **59** with thiol-functionalized glass **29**. The reaction conditions were adjusted in a way that glass **29** substituted only one of the bromo groups on the perylene ring. Therefore, 1.5 molar equivalent of **29** was used and the reaction was carried out at room temperature to prevent as much as possible the formation of compound **60**.

After stirring at room temperature for three days, the reaction mixture was monitored by TLC, showing the desired product, along with small amounts of unreacted starting material and disubstituted derivative **60**. The crude product was

purified by filtration on a short silica plug using CH<sub>2</sub>Cl<sub>2</sub> then CH<sub>2</sub>Cl<sub>2</sub>/AcOEt 4:1 as eluent, giving pure compound **61** in 69% yield. The product was characterized by NMR spectroscopy, HRMS and FTIR. The peaks at 9.64 and 9.04 ppm in the <sup>1</sup>H NMR spectrum correspond to the two protons neighboring the bromine atom. Each of these two peaks integrates for one proton while in the case of the 1,7-dibromo precursor (**59**) these two peaks each integrate for two protons. This means that there is only one bromine substituent on the perylene ring and the other bromine atom has effectively been substituted with the sulfide group. The two protons on the PDI unit neighboring the sulfide group present a doublet and a singlet at 8.68 and 8.38 ppm respectively and each integrating for one proton. Also, the -NH peak at 6.97 ppm, which corresponds to the -NHMe group, integrates for two protons for the case of compound **60** while this peak integrates for one proton in the <sup>1</sup>H NMR spectrum of compound **61**. The chemical shifts of the glass proton peaks are also shifted as a result of their attachment to the PDI dye. As an example, the aryl protons *ortho* to the thiol group in precursor **29** present a doublet at 7.66 ppm that integrates for two protons. The shift from 7.66 ppm to 7.93 ppm in compound **60** is indicative of the different environment that the protons are in. HRMS further confirmed the identity of compound **60**.

The remaining bromo group of compound **61** could be further substituted with other functional groups in order to tune the electronic properties of the dye. One such example is substitution with pyrrolidine, which is performed at ambient temperature in the presence of an excess of pyrrolidine and K<sub>2</sub>CO<sub>3</sub> to give compound **62** in 74 % yield. Compound **62** shows a deep green color in contrast to the burgundy color of compound **61**. After purification of the desired product on a silica plug using DCM/EtOAc (4:1), a sample of pure product was submitted for characterization by NMR spectroscopy. The disappearance of the peak at 9.5 ppm indicates that the remaining bromine atom was substituted, and the appearance of two peaks at 3.36 (4H) and 2.06 (4H) is evidence of the presence of the pyrrolidine ring. Pyrrolidine protons normally show up at 1.7 and 2.8 ppm, although in this case, the peaks are shifted to higher values as a consequence of being bonded to the perylene group.

In addition, an attempt was made to substitute the remaining bromine group of compound **61** with thiophenol, in order to have an isoelectronic analogue of compound **59** but with only one methylaminotriazine unit. The reaction was performed under the same conditions used to synthesize compound **63**, and a deep red solid was obtained. The major product was purified on silica using DCM/EtOAc (9:1). The identity of the compound was confirmed with HRMS, and while the product appeared to be pure by TLC and HRMS, the integrations of some <sup>1</sup>H NMR peaks did not match the expected number of protons. By repeating the reaction procedure and trying other experimental procedures, this observation will be investigated.

### 2.2.2. Optical Properties

From a structural viewpoint, the synthesized PDI-functionalized molecular glasses are polycyclic compounds containing conjugated systems of electrons. Due to the presence of conjugated chromophores and resulting  $\pi \rightarrow \pi^*$  transitions, the delocalized electrons show absorption in the visible range of the electromagnetic spectrum. As lateral substituents vary in the structures of these compounds, the intensity and the position of absorption maxima are changed accordingly.

The UV-Vis spectra of PDI glasses **60-62** were recorded in both dichloromethane solution and in the solid state in order to compare the absorption of the various chromophores as well as the shifts in the solid state representative of molecular aggregation. Solid films of the candidates were prepared by spin-coating from dichloromethane or THF solution, and in all cases the compounds formed uniform glassy films from solution after evaporation of the solvent. Absorption spectra for both solution and solid state are shown in Figures 4 and 5, respectively, and absorption maxima and extinction coefficients are reported in Table 2.

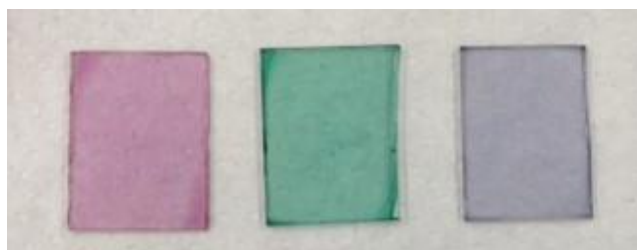


Figure 3: Thin films of PDI-functionalized molecular glasses prepared by spin-coating from  $\text{CH}_2\text{Cl}_2$  or THF solution. From left to right: **61**, **62**, **60**.

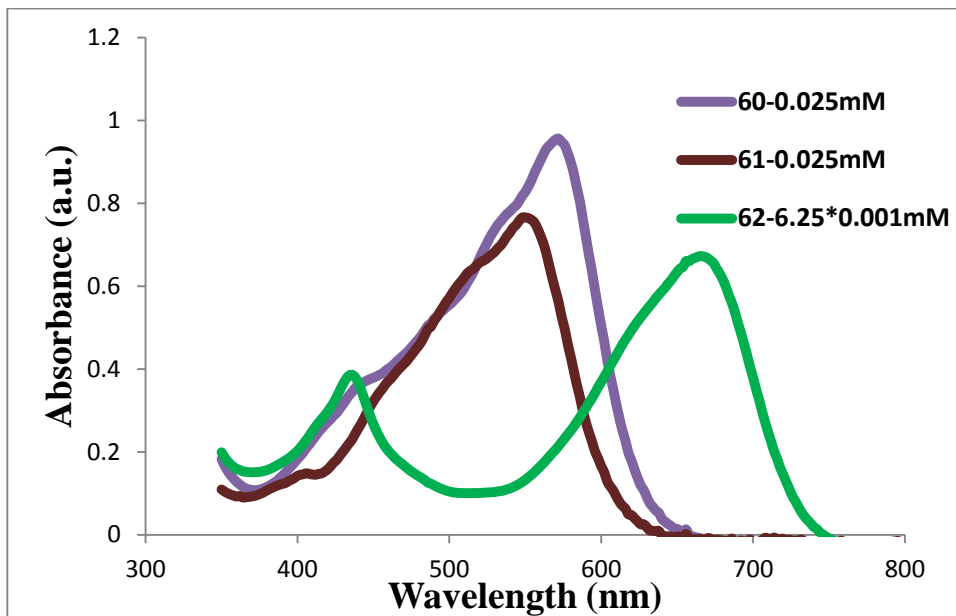


Figure 4: UV-Vis absorption spectra of PDI-functionalized molecular glasses in  $\text{CH}_2\text{Cl}_2$  solution.

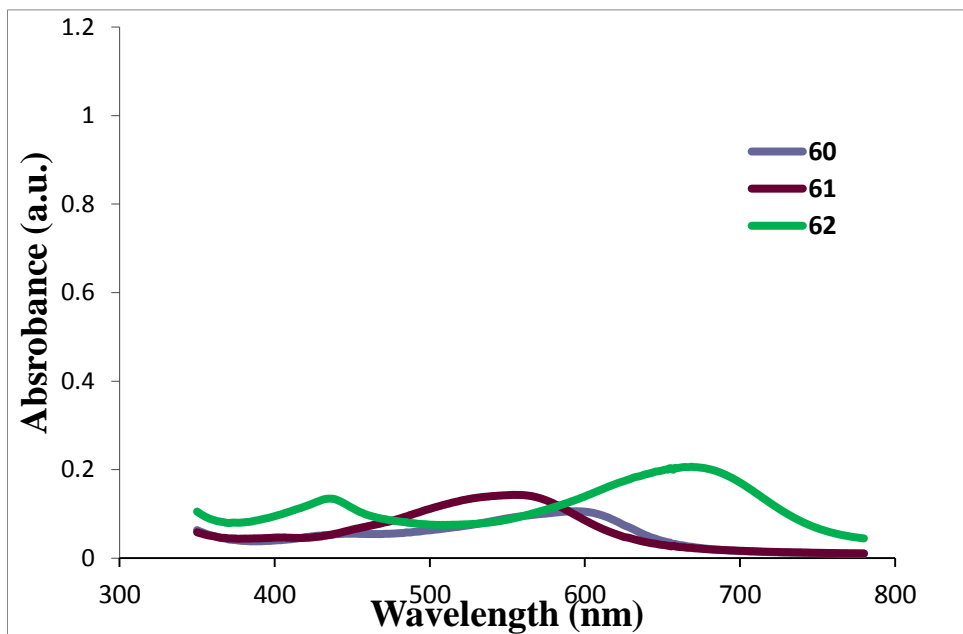


Figure 5: UV-Vis absorption spectra of PDI-functionalized molecular glasses deposited from  $\text{CH}_2\text{Cl}_2$  or THF as thin films.

Table 2: UV-Vis absorbance values of PDI functionalized molecular glasses in solution and in the solid state.

Compound	$\lambda_{\max}$ in solution (nm)	$\epsilon$ (extinction coefficient) in solution ( $\text{cm}^{-1} \text{M}^{-1}$ )	$\lambda_{\max}$ in solid (nm)
<b>60</b>	570	38000	595
<b>61</b>	548	30400	554
<b>62</b>	664	107200	668

The absorption spectrum of bis(mexylaminotriazinyl) dye **60** shows an intense absorption in the visible region of the spectrum, with absorption reaching a maximum at  $\lambda=570$  nm in solution and at 595 nm in the solid state, whereas for monosubstituted analogue **61**, the absorption maximum is slightly shifted to a shorter wavelength (548 nm in solution and 554 nm in the solid state). This hypsochromic shift results from the presence of only one sulfide group on the chromophore in compound **61**. The  $\lambda_{\max}$  values for compound **62** were found at 664 nm in solution and at 668 nm in the solid state. While the absorption maxima between solution and the solid state are nearly identical for monotriazinyl compounds **61-62**, the shift observed in the case of compound **60** is more significant, hinting to the presence of a higher degree of aggregation in the solid state. The second mexylaminotriazine unit in compound **60** therefore seems to favor the alignment of perylene groups in the solid state to a higher extent than compounds **61-62**. Proper alignment of electron transporting groups is crucial for device performance.

One important issue to obtain high performance devices that should be considered is controlling the molecular alignment of PDI-based materials which leads to improved electron mobility in films. Hindered bay substituents, or bulky imide substituents, can limit the  $\pi$ - $\pi$  stacking of units, leading to a lower degree of aggregation between the perylene units in the solid state. Such poor packing would decrease the device performance. Substituting the imide parts of the molecule with molecular glasses instead of the bay region would bring the conjugated system closer together and facilitate the interaction of PDI units. In addition, replacing the bulky 2,6-diisopropylphenyl groups with linear alkyl groups would decrease the

steric hinderance around the perylene ring systems and improve the alignment of the units.

On the other hand, the UV-Vis spectrum of pyrrolidine-functionalized dye **62** shows a significant change in absorption maximum compared to the other two derivatives **60** and **61** (Figure 4). This observation can be explained by the strong electron-donating nature of the pyrrolidine substituent that impacts the intensity of absorption, the position of absorption maxima and the extent of shift. Similar observations have already been made with perylenediimide dyes substituted by amines in the bay region.<sup>64</sup>

It can be observed by comparing the absorption spectra of PDI-functionalized molecular glasses that the absorption bands are shifted to different wavelengths by modifying the substituents. The presence of substituents carrying delocalized electrons attached on the structure of PDI units decreases the energy required for electronic excitation and increases the extent of conjugation in the  $\pi$  system of the molecule. This results in a red shift of the curve and moves the absorption maximum to a higher value. For the case of compound **60**, the addition of a second triazine favors the aggregation in the solid state to a higher extend, resulting in a larger shift of absorption maxima in the solid state compared to solution, but at the cost of lower solubility in most solvents.

### 2.2.3. Thermal Properties

As expected, the mexylaminotriazine moiety imparted its glass-forming ability to the PDI dyes as presented in the diagrams in Figures 16-18. It should be noted that repeated heating cycles above 200°C resulted in different  $T_g$  values between different cycles, hinting that decomposition takes place upon prolonged heating at high temperatures. This was confirmed by <sup>1</sup>H NMR spectroscopy. As the  $T_g$  values for these compounds are very high, repeated analyses had to be performed with different samples to validate the results.

DSC analysis of compound **60** presents a clear evidence of a glass transition at approximately 210 °C. Compound **61** shows a slightly lower  $T_g$  of 206 °C, while compound **62** presents the lowest  $T_g$  in the group (186 °C), potentially as a result of the more flexible pyrrolidine ring. One possible explanation for the slightly higher glass transition temperature observed for compound **60** compared to glasses **61-62** is the presence of stronger intermolecular interactions as the result of the two triazine groups attached to the PDI unit, and higher molecular weight. However, it is obvious that the large PDI moiety impacts  $T_g$  more strongly than the triazine group in this series of compounds.

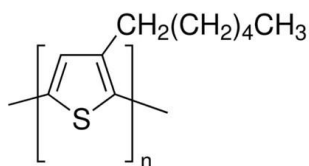
#### 2.2.4. Photovoltaic Properties

The synthesized PDI dyes share a similar electronic structure based on  $\pi$ -conjugated electrons. Due to the high electronic mobility, low lying LUMO and high molar absorption coefficient characteristic of PDI dyes, and the solubility and processability introduced by the triazine group, such candidates are considered promising *n*-type electron acceptors in optoelectronic fields.

In addition, perylenediimides have a strong light-harvesting ability and absorb in a significant portion of the visible range (400-600 nm). This property is advantageous for organic photovoltaics, compared to the most common acceptors (fullerenes) that absorb only slightly in the visible range, which makes perylene diimides excellent acceptor candidates for organic solar cell applications.<sup>65</sup>

In order to investigate the photovoltaic properties of the synthesized candidates, bulk heterojunction (BHJ) photovoltaic cells were fabricated in the Nunzi research group at Queen's University using compounds **61** and **62** as electron acceptors paired with P3HT **64** as electron donor. The absorption spectra for the chosen donor polymers are complementary with that of PDI dyes in films. In addition, the P3HT polymers was selected because of high hole mobility and affordability, and because of the abundance of literature published with it. High-boiling dichlorobenzene was selected as the solvent to spin coat the films so that polymer molecules can align and order properly within the film. Another reason to choose dichlorobenzene as the solvent is that both the polymer and the glass show appreciable solubility in it.

For the case of compound **61**, the structure of the optimal device fabricated was ITO/ZnO/P3HT: **61** /PEDOT:PSS/Ag (100 nm) with P3HT: **61** (2:1) and the obtained power conversion efficiency was 0.22%.



**64**

Scheme 14: P3HT used as donor polymer in photovoltaic cell.

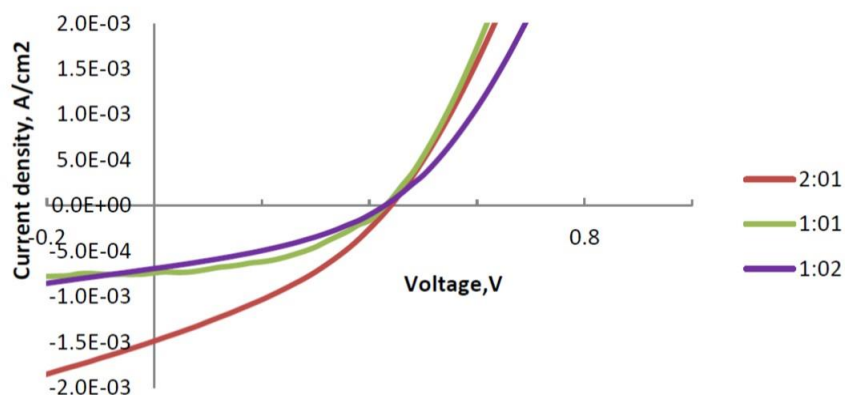


Figure 6: I-V curves of photovoltaic cells of compound **61** with P<sub>3</sub>HT obtained from three different ratios (2:1, 1:1, 1:2).

Table 3: Photovoltaic parameters of photovoltaic cells of compound **61** with P<sub>3</sub>HT.

Device	J <sub>sc</sub> (mAcm <sup>-2</sup> )	V <sub>oc</sub> (V)	FF (%)	R <sub>sh</sub> (Ohm)	R <sub>s</sub> (Ohm)	PCE (%)
2:1	1.49	0.44	34.2	2.4E+03	6.6E+02	0.22

The device fabricated with P<sub>3</sub>HT: **62** (2:1) and the structure of ITO/ZnO/P<sub>3</sub>HT: **62**/MoO<sub>3</sub> (3nm)/Ag (100 nm) yielded a conversion efficiency of 0.2%. Since compound **60** seems to aggregate better in the solid state, it is expected to have the highest performance among the group in BHJ photovoltaic cells. However, due to its low solubility in most organic solvents, it was impossible to find a suitable solvent that could properly dissolve it and the polymer, and therefore it was not tested.

Although low conversion efficiencies were obtained from preliminary tests, these results are nonetheless promising because they show that glass-forming PDI derivatives can be successfully used in bulk heterojunction photovoltaic cells. They will have to be improved by optimizing the structure of the acceptor PDI glass, the donor polymer, and device fabrication conditions. The structure of the acceptor PDI glass can be improved by improving the  $\pi$ - $\pi$  stacking between the

PDI units. This can be done by replacing the large 2,6-diisopropylphenyl groups with smaller groups. While these groups greatly improve the solubility of the PDI derivatives, because the phenyl groups are twisted relative to the perylene ring system, the isopropyl groups are located directly above and below the perylene group, thereby preventing the perylene units from packing efficiently. Replacing the PDI end groups with linear alkyl chains would decrease the hindrance. Incorporation of conjugated functional groups in the bay position could facilitate the transport of electrons. In addition, bay substituents with minimal steric demand would limit the twisting of the PDI units and increase the chance of proper alignment and charge transport between the units. Care must also be taken to ensure that the compounds show a high resistance to crystallization and appreciable solubility in most solvents.

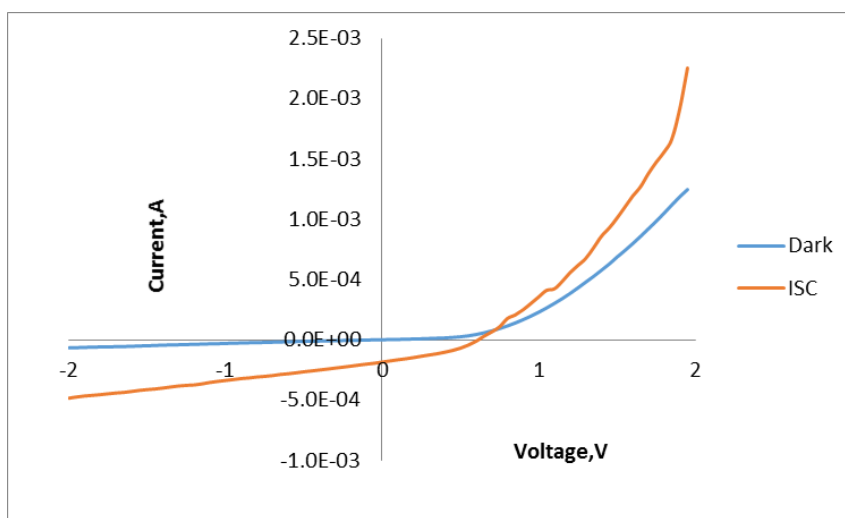


Figure 7: I-V curves of photovoltaic cells of compound **62** with P3HT.

Table 4: Photovoltaic parameters of photovoltaic cells of compound **62** with P3HT.

Isc(A)	Voc(V)	FF (%)	R <sub>SH</sub> (Ohm)	R <sub>S</sub> (Ohm)	PCE (%)
-185.3E-6	600E-3	0.37	834.88	650.1	0.2

## 2.3. Experimental

### 2.3.1. Materials and Equipment

3, 4, 9, 10-Perylenetetracarboxylic dianhydride, iodine, bromine, sulphuric acid, 2,6-diisopropylaniline, propanoic acid, cetyltrimethylammonium bromide, pyrrolidine, and K<sub>2</sub>CO<sub>3</sub> (potassium carbonate) were purchased from commercial sources and used without further purification. Solvents (toluene, acetone, ethyl acetate, THF (tetrahydrofuran), DCM (dichloromethane) and methanol) were purchased from Caledon Laboratories and used without further purification. DMSO-*d*<sub>6</sub> (deuterated dimethyl sulfoxide) was purchased from CDN isotopes. Chromatography was performed using Silia Flash P60 grade silica gel purchased from SiliCycle. Compound **58**,<sup>61</sup> **59**,<sup>61</sup> **29**,<sup>21</sup> were synthesized according to a literature procedure. <sup>1</sup>H NMR spectra were recorded on a Bruker AV-400 spectrometer at 400.3 MHz. <sup>13</sup>C NMR spectra were on Varian Oxford spectrometer at 75 MHz. FTIR spectra were recorded on a Elmer Spectrum GX Sspectrometer as thin films on KBr disks deposited from THF or CH<sub>2</sub>Cl<sub>2</sub>. Thermal analysis was obtained by DSC performed on a TA Instruments 2010 apparatus calibrated with indium at a heating rate of 5 °C/min. Analyses were repeated on at least two separate samples. UV-Vis studies were performed by Agilent Hewlett-Packard 8453A spectrophotometer.

### 2.3.2. Synthesis

#### 2.3.2.1. Synthesis of Compound 59

Perylene bisanhydride (20.0 g, 50.9 mmol) was added to concentrated sulphuric acid (300 mL) and the mixture was heated for 20 h at 55 °C, and subsequently iodine (0.516 g, 2.00 mmol) was added and the mixture was heated for additional 5 h at 55 °C. Next, bromine (18.3 g, 5.90 mL, 114 mmol) was added to the mixture dropwise. After addition of bromine, the reaction mixture was heated for 48 h at 85 °C. The flask was cooled down to room temperature and the excess amount of bromine was removed by gentle flow of nitrogen gas. Water (40 mL) was added to the reaction mixture slowly and the resulted precipitate was filtered, washed with concentrated sulphuric acid (200 mL) and large amounts of water to yield an orange powder (Scheme 8) which was taken directly to the next step.

A mixture of crude compound **58** (15.0 g, 27.0 mmol) and 2,6-diisopropylaniline (48.34 g, 51.4 mL, 272 mmol) in propanoic acid (250 mL) was

refluxed for 3 days (Scheme 9). This reaction was maintained under nitrogen atmosphere. After the reaction mixture was cooled down to room temperature, methanol (600 mL) was added and the resulted precipitate was separated by filtration and washed with methanol (50 mL) to yield an orange product (6.49 g, 28%). <sup>1</sup>H NMR (300 MHz, CDCl<sub>3</sub>, 298 K): δ 9.56 (d, <sup>3</sup>J=8.2 Hz, 2H), 9.02 (s, 2H), 8.81 (d, <sup>3</sup>J=7.9 Hz, 2H), 7.51 (m, 2H), 7.36 (d, <sup>3</sup>J=7.6 Hz, 4H), 2.74 (m, 4H), 1.19 (d, <sup>3</sup>J=6.7 Hz, 24H).

### 2.3.2.2. Synthesis of Compound 60

In a round bottom flask equipped with a magnetic bar, was stirred a mixture of toluene (200 mL), water (125 mL), potassium carbonate (4.22 g, 30.0 mmol) and cetyltrimethylammonium bromide (0.265 g, 1.90 mmol) under nitrogen atmosphere for 15 min at room temperature. Compound **59** (2.65 g, 3.05 mmol) and compound **29** (3.23 g, 9.15 mmol) were added and the reaction mixture was heated at 80 °C overnight. After the reaction mixture was cooled down to room temperature, the product was isolated from the solution by filtration and washed with toluene (50 mL), water (50 mL), and acetone (20 mL). The purple solid was allowed to dry in a vacuum and afforded 3.35 g product (2.37 mmol, 77%). T<sub>g</sub> 211 °C; FTIR (CH<sub>2</sub>Cl<sub>2</sub>/KBr) 3411, 3324, 3195, 3075, 2962, 2921, 2870, 1699, 1664, 1606, 1594, 1583, 1568, 1553, 1511, 1501, 1492, 1456, 1442, 1427, 1412, 1389, 1365, 1335, 1312, 1295, 1263, 1248, 1236, 1213, 1197, 1184, 1148, 1095, 1056, 1038, 1012, 998, 970, 937, 922, 885, 856, 836, 809, 795, 742, 715, 702, 662 cm<sup>-1</sup>; <sup>1</sup>H NMR (400 MHz, DMSO-*d*<sub>6</sub>, 363 K): δ 9.50 (br s, 1H), 9.36 (br s, 1H), 9.08 (br s, 1H), 8.91 (br s, 1H), 8.79 (br s, 4H), 8.29 (br s, 2H), 8.00 (br s, 4H), 7.51 (br d, 4H), 7.43 (br t, 2H), 7.31 (br m, 8H), 6.97 (br s, 2H), 6.53 (s, 2H), 2.8 (br s, 6H), 2.7 (m, 4H), 2.13 (s, 12H), 1.03 (br d, 24 H) ppm; <sup>13</sup>C NMR (75 MHz, DMSO-*d*<sub>6</sub>): δ 166.0, 164.0, 163.7, 162.84, 162.76, 145.3, 142.8, 140.2, 139.7, 137.0, 135.6, 131.9, 131.3, 130.5, 129.2, 128.7, 128.4, 127.9, 125.4, 123.7, 123.2, 122.0, 121.3, 121.2, 120.6, 117.8, 28.5, 27.2, 23.6, 21.0 ppm; HRMS (MALDI, MH<sup>+</sup>) calcd. for C<sub>84</sub>H<sub>79</sub>N<sub>14</sub>O<sub>4</sub>S<sub>2</sub> (*m/e*): 1411.5850, found: 1411.5866

### 2.3.2.3. Synthesis of Compound 61

A mixture of THF (800 mL) and K<sub>2</sub>CO<sub>3</sub> (11.1 g, 80.0 mmol) was stirred and deoxygenated under nitrogen atmosphere for 30 min. Next, compound **59** (14.0 g, 16.0 mmol) and glass **29** (8.52 g, 24.0 mmol) were added and the reaction mixture was stirred at room temperature for 3 days. THF was removed under reduced pressure and the crude product was purified on a short silica pad eluting with 100% dichloromethane initially to remove unreacted starting material. After collecting the fractions containing the starting material, the eluent was switched to DCM/EtOAc

(80:20). 12.6 g of a pure dark red product was obtained (11.1 mmol, 69%).  $T_g$  206 °C; FTIR (CH<sub>2</sub>Cl<sub>2</sub>/KBr) 3420, 3346, 3195, 3102, 3065, 3027, 2964, 2930, 2869, 1709, 1669, 1621, 1586, 1559, 1538, 1518, 1497, 1457, 1444, 1430, 1413, 1388, 1363, 1335, 1306, 1242, 1198, 1181, 1148, 1094, 1057, 1040, 1013, 995, 969, 937, 919, 885, 859, 838, 809, 793, 770, 749, 741, 714, 698, 668 cm<sup>-1</sup>; <sup>1</sup>H NMR (400 MHz, DMSO-*d*<sub>6</sub>, 363 K): δ 9.64 (d, <sup>3</sup>*J*=8.0 Hz, 1H), 9.04 (br s, 1H), 8.86 (m, 3H), 8.70 (d, <sup>3</sup>*J*=8.0 Hz, 1H), 8.56 (br s, 1H), 8.38 (br s, 1H), 7.93 (d, <sup>3</sup>*J*=8.0 Hz, 2H), 7.47 (m, 4H), 7.36 (d, <sup>3</sup>*J*=4.0 Hz, 2H), 7.32 (d, <sup>3</sup>*J*=4.0 Hz, 2H), 7.29 (s, 2H), 6.63 (br s, 1H), 6.57 (s, 1H), 2.85 (s, 3H), 2.8 (m, 2H), 2.71 (m, 2H), 2.18 (s, 6H), 1.14 (d, <sup>3</sup>*J*=2.0 Hz, 6H), 1.12 (d, <sup>3</sup>*J*=2.4 Hz, 6H), 1.08 (d, <sup>3</sup>*J*=8.0 Hz, 6H), 1.04 (d, <sup>3</sup>*J*=8.0 Hz, 6H) ppm; <sup>13</sup>C NMR (75 MHz, DMSO-*d*<sub>6</sub>): δ 165.9, 163.9, 163.6, 162.6, 162.1, 145.4, 145.2, 142.7, 142.6, 140.8, 140.7, 139.7, 137.1, 136.9, 135.3, 132.6, 132.3, 131.9, 131.7, 130.4, 129.3, 128.9, 128.6, 128.4, 128.2, 127.9, 127.0, 125.5, 123.7, 123.2, 122.2, 122.0, 121.6, 121.5, 120.5, 119.9, 117.8, 28.4, 27.2, 23.6, 21.0 ppm; HRMS (MALDI, MH<sup>+</sup>) calcd. for C<sub>66</sub>H<sub>60</sub>BrN<sub>8</sub>O<sub>4</sub>S (*m/e*): 1139.3642, found: 1139.3649.

#### 2.3.2.4. Synthesis of Compound 62

In a round bottom flask equipped with a magnetic stirrer, compound **61** (0.590 g, 0.517 mmol) was dissolved in pyrrolidine (2.50 mL) followed by addition of THF (2.50 mL) and K<sub>2</sub>CO<sub>3</sub> (0.078 g, 0.50 mmol). The reaction mixture was stirred at room temperature for 2 days. The volatiles were removed under reduced pressure and the crude product was purified on a short silica pad with DCM/EtOAc (80:20) as eluent. The fractions containing the desired product were collected and the solvent was removed under reduced pressure to yield 0.431 g pure green product (0.380 mmol, 74%).  $T_g$  186 °C; IR (DCM/KBr) 3915, 3846, 3821, 3739, 3689, 3659, 3621, 3551, 3349, 3193, 3070, 2961, 2930, 2915, 2868, 1700, 1667, 1606, 1593, 1579, 1556, 1496, 1423, 1403, 1381, 1363, 1336, 1290, 1239, 1201, 1181, 1152, 1132, 1119, 1057, 1014, 965, 940, 917, 838, 809, 795, 773, 753, 739, 714, 691, 668, 601, 582, 537 cm<sup>-1</sup>; <sup>1</sup>H NMR (400 MHz, DMSO-*d*<sub>6</sub>, 363.15 K): δ 9.01 (br s, 1H), 8.99 (br s, 1H), 8.65 (d, <sup>3</sup>*J*=8.0 Hz, 1H), 8.59 (s, 1H), 8.53 (d, <sup>3</sup>*J*=8.0 Hz, 2H), 8.40 (s, 1H), 7.88 (d, <sup>3</sup>*J*=8.0 Hz, 2H), 7.65 (d, <sup>3</sup>*J*=8.0 Hz, 1H), 7.47 (m, 2H), 7.41 (d, <sup>3</sup>*J*=8.0 Hz, 2H), 7.35 (d, <sup>3</sup>*J*=8.0 Hz, 2H), 7.29 (m, 4H), 6.61 (br s, 1H), 6.53 (s, 1H), 3.36 (br s, 4H), 2.85 (d, <sup>3</sup>*J*=1.0 Hz, 3H), 2.78 (m, 2H), 2.68 (m, 2H), 2.14 (br s, 6H), 2.06 (br s, 4H), 1.13 (d, 12H), 1.08 (d, <sup>3</sup>*J*=8.0 Hz, 6H), 1.04 (d, <sup>3</sup>*J*=8.0 Hz, 6H); <sup>13</sup>C NMR (75 MHz, DMSO-*d*<sub>6</sub>): 165.9, 163.9, 163.6, 163.48, 163.41, 163.04, 162.8, 148.2, 145.4, 145.2, 141.9, 139.8, 137, 135.7, 134.6, 133.5, 131.4, 130.9, 130.8, 130.2, 129.3, 129.1, 128.4, 126.1, 125.5, 124.2, 123.7, 123.1, 122.2, 121.9, 121.7, 121.5, 120.5, 119.9, 117.7, 116.9, 114.1, 52.6, 28.5, 27.2, 25.3,

20.9 ppm. HRMS (MALDI, MH<sup>+</sup>) calcd. for C<sub>70</sub>H<sub>68</sub>N<sub>9</sub>O<sub>4</sub>S (*m/e*): 1130.43, found: 1130.5114.

### 2.3.2.5. Synthesis of Compound 63

THF (20 mL) and K<sub>2</sub>CO<sub>3</sub> (0.606 g, 4.38 mmol) were added together and deoxygenated by bubbling nitrogen gas through the solution for 15 min. Next, thiophenol (0.193 g, 0.179 mL, 1.75 mmol) and compound **61** (1g, 0.877 mmol) were added and the reaction mixture was stirred for 3 days (Scheme 13). After removing the volatiles under reduced pressure, the crude product was purified on a silica column with DCM/EtOAc (90:10). The fractions containing the desired product were joined and the solvent was removed under reduced pressure to yield 0.688 g of a red product. This product was characterized by <sup>1</sup>H NMR spectroscopy. HRMS (MALDI, MH<sup>+</sup>) calcd. for C<sub>72</sub>H<sub>65</sub>N<sub>8</sub>O<sub>4</sub>S<sub>2</sub> (*m/e*): 1130.4570, found: 1130.4562.

## 2.4. Summary

Mexylaminotriazine molecular glasses functionalized with perylenediimide (PDI) dyes were synthesized successfully with good overall yields, and the products showed the ability to readily form long-lived glasses. The candidates were characterized by NMR spectroscopy and HRMS. The bromination of 3,4,9,10-perylenetetra-carboxylic dianhydride followed by imidization by 2,6-diisopropylaniline afforded a 1,7-dibromoperylene-diimide intermediate that was used as a common precursor to synthesize glass-functionalized PDI dyes. The introduction of mexylaminotriazine groups through a thiol functionality and other functional groups such as pyrrolidine on the perylene ring improved the solubility and facilitated the process of purification and characterization. The T<sub>g</sub> of the candidates was measured by DSC and they proved to be capable of making uniform thin films. In addition, the photovoltaic properties of candidates were investigated by fabricating photovoltaic cells using selected candidates as electron acceptors. Preliminary tests were performed and promising results were obtained for synthesized glass-functionalized PDI dyes. Although power conversion efficiencies of less than 1% were obtained, proper optimization of the device fabrication conditions and of the PDI glass structure should yield improved results.

## 2.5. Appendix

### 2.5.1. NMR Figures

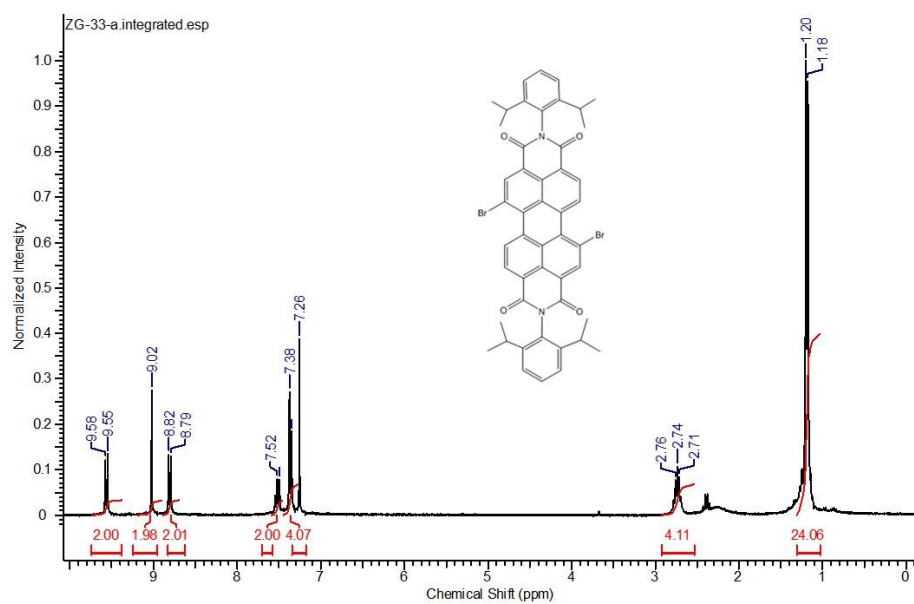


Figure 8:  $^1\text{H}$  NMR spectrum of compound **59**, in  $\text{CDCl}_3$ , 300 MHz.

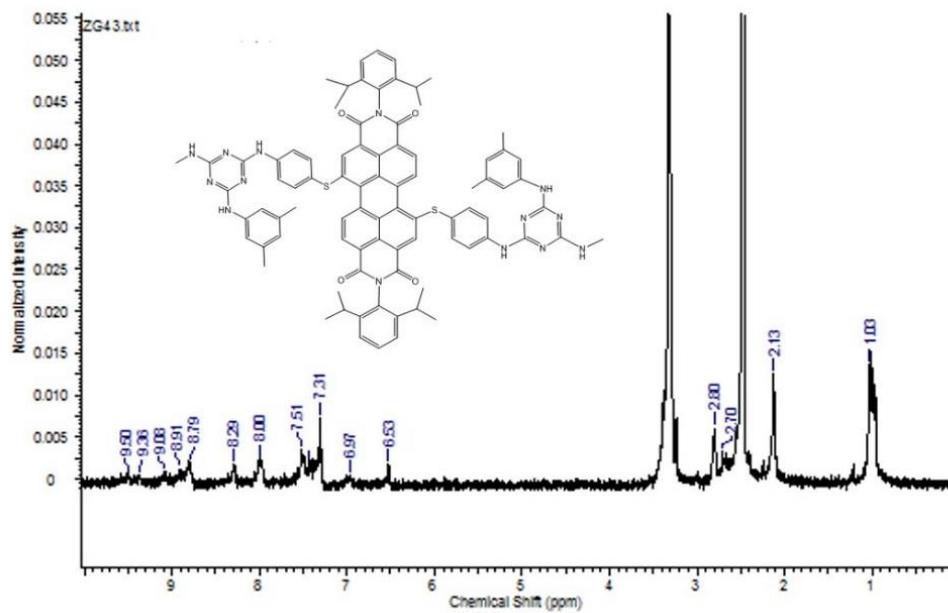


Figure 9:  $^1\text{H}$  NMR spectrum of compound **60** in  $\text{DMSO}-d_6$ , 400 MHz.

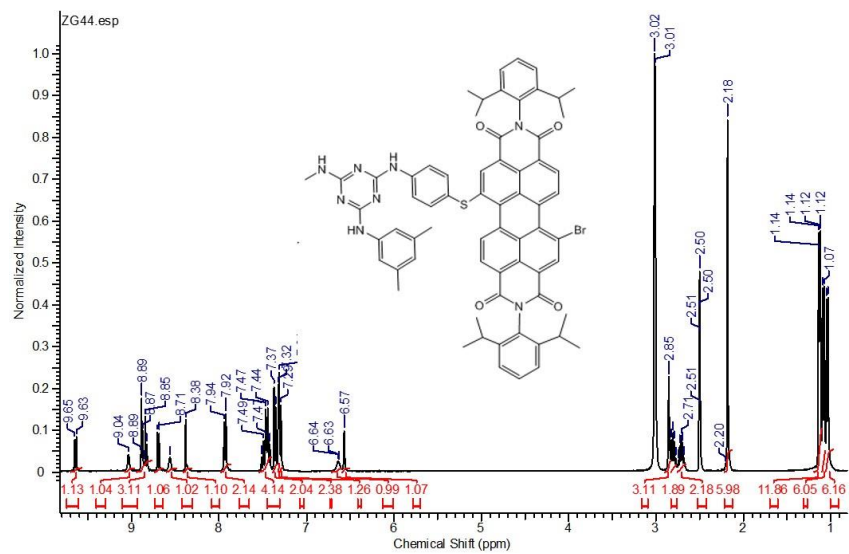


Figure 10:  $^1\text{H}$  NMR spectrum of compound **61** in  $\text{DMSO}-d_6$ , 400 MHz.

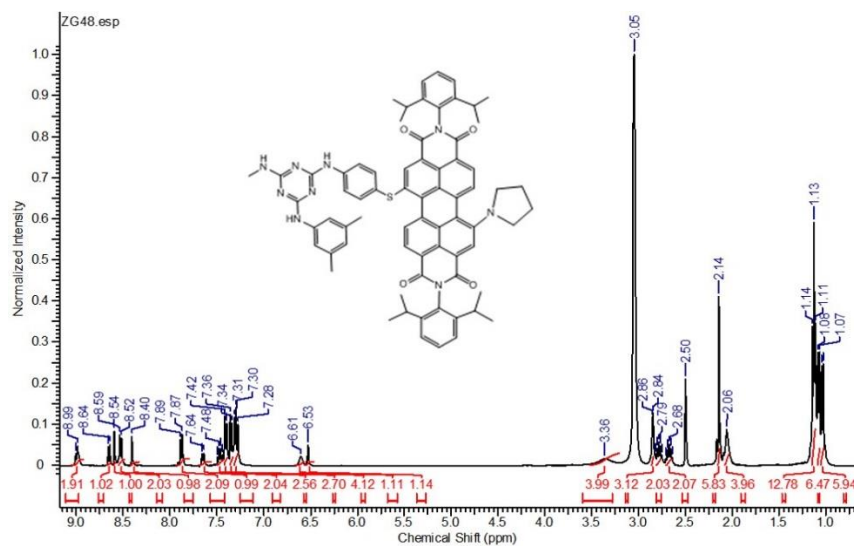


Figure 11:  $^1\text{H}$  NMR spectrum of compound **62** in  $\text{DMSO}-d_6$ , 400 MHz.

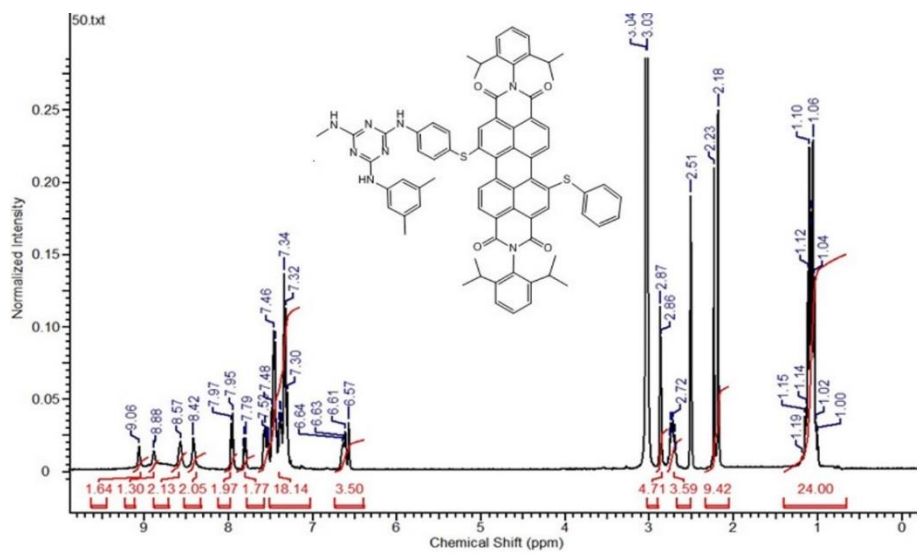


Figure 12:  $^1\text{H}$  NMR spectrum of compound **63** in  $\text{DMSO}-d_6$ , 400 MHz.

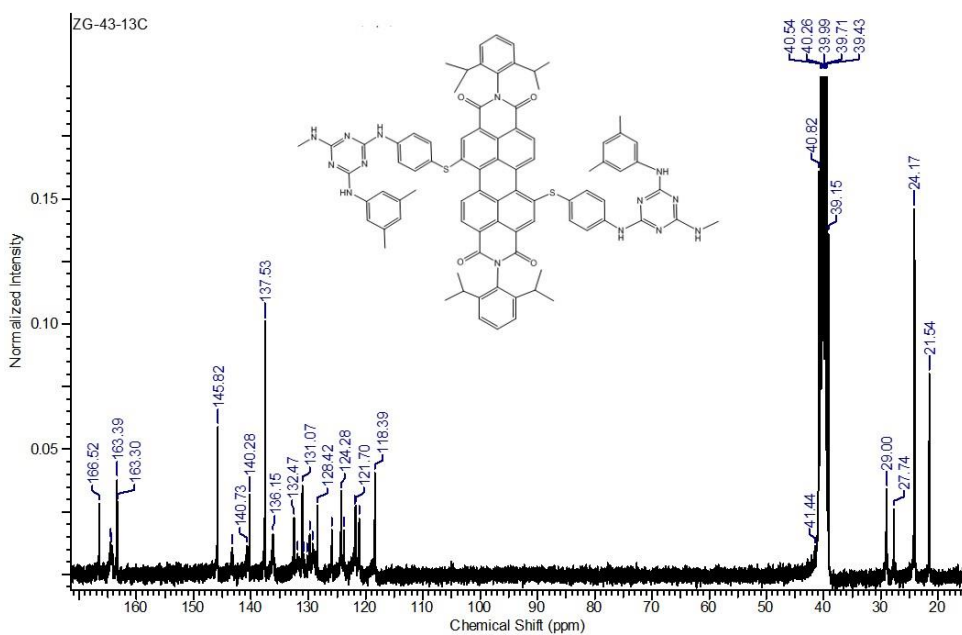


Figure 13:  $^{13}\text{C}$  NMR spectrum of compound **60** in  $\text{DMSO}-d_6$ , 75 MHz.

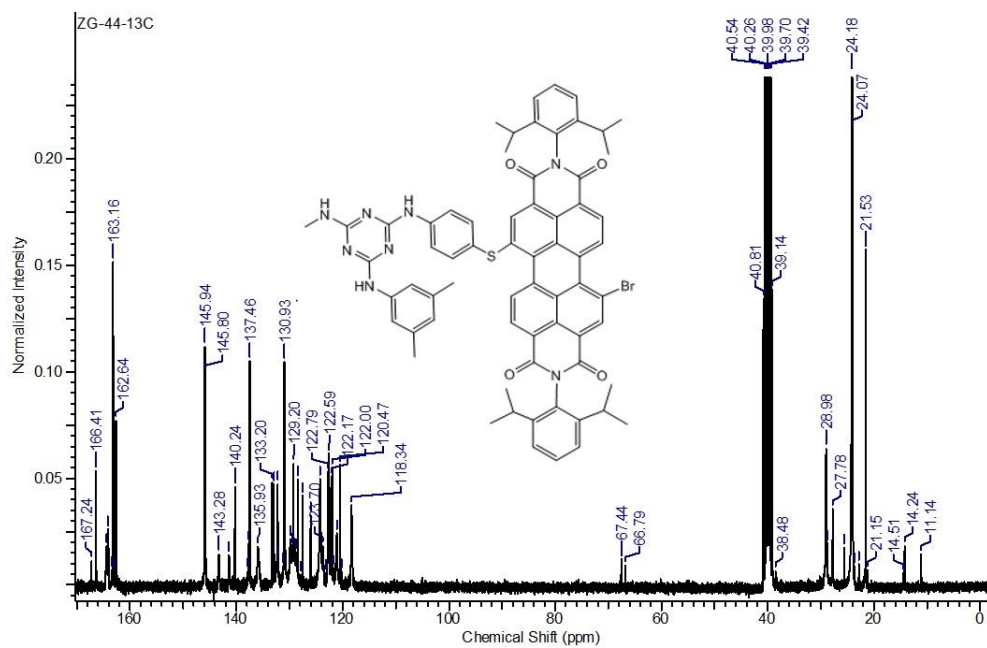


Figure 14:  $^{13}\text{C}$  NMR spectrum of compound **61** in  $\text{DMSO-}d_6$ , 75 MHz.

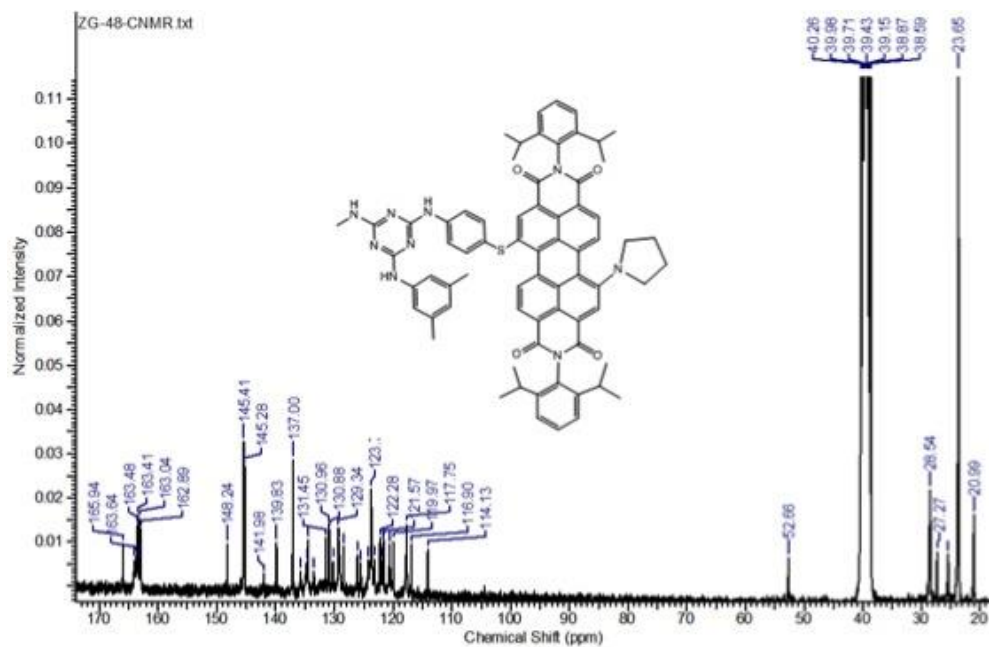


Figure 15:  $^{13}\text{C}$  NMR spectrum of compound **62** in  $\text{DMSO-}d_6$ , 75 MHz.

## 2.5.2. DSC Thermograms

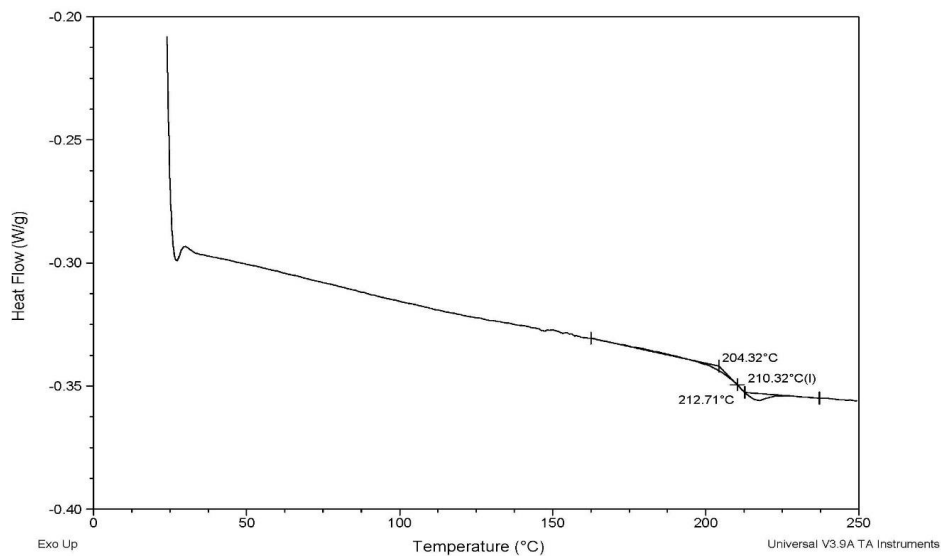


Figure 16: DSC analysis of compound **60**.

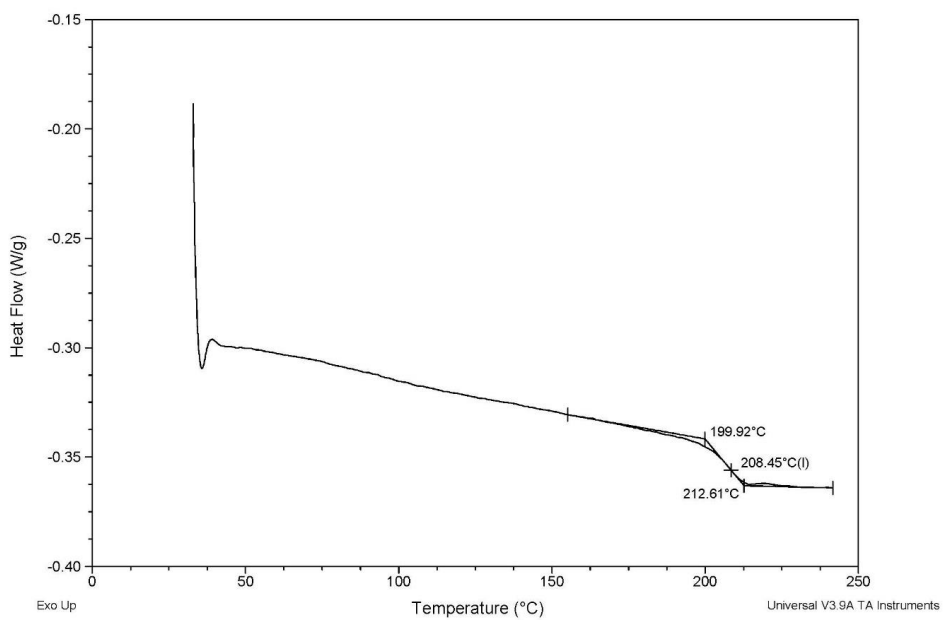


Figure 17: DSC analysis of compound **61**.

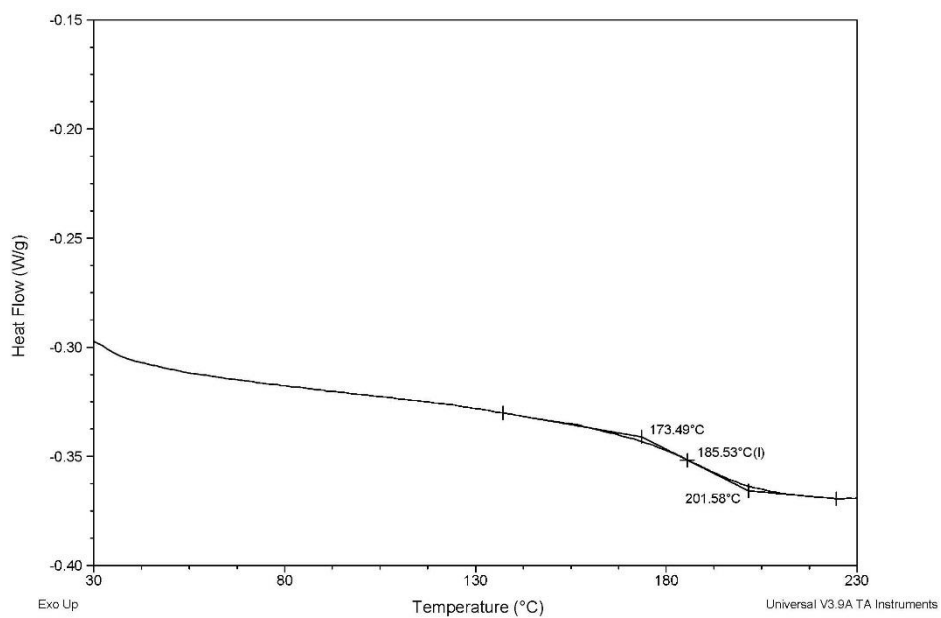


Figure 18: DSC analysis of compound **62**.

## **3 Fullerene Functionalized Molecular Glasses**

### **3.1. Introduction**

#### **3.1.1. Definition and Properties of Fullerene Dyes**

Organic solar cells are used as a platform for the conversion of solar energy, as an alternative to fossil fuels.<sup>41</sup> Fullerene derivatives have been proved to be *n*-type semiconductors which work as strong electron acceptors in PV cells. Undoubtedly, fullerene derivatives have been the most successful acceptors in organic solar cells and due to substantial chemical modification on the structure of fullerenes, the LUMO energy levels have increased during the past decade.<sup>66</sup> In addition to PV cells, films of fullerene derivatives have applications as active elements of thin film transistors.<sup>67</sup>

#### **3.1.2. Applications**

Fullerene and its derivatives continue to attract the attention of scientists because of their unique electronic properties and applications in several fields.<sup>68</sup> Many chemical reactions have been developed to synthesize various fullerene structures with outstanding magnetic, electrochemical, superconducting, photophysical and structural properties.<sup>69</sup>

In addition to their chemical, physical and photophysical properties, various device applications were discovered when solid films of fullerenes were studied. In order to facilitate the formation of uniform and high-quality thin films from fullerene derivatives that are easy to process, the formation of amorphous phases of fullerenes would be desirable. Therefore, in such cases, the ability of thin films to resist crystallization from the amorphous state would be desirable.<sup>70</sup> For this purpose, methylaminotriazine glasses can be used as platforms to functionalize with fullerenes in order to induce glass-forming properties in the latter.

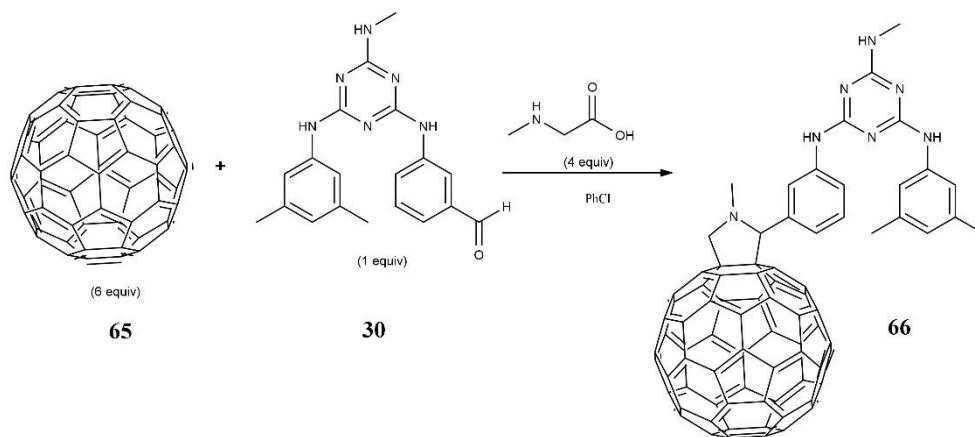
#### **3.1.3. Potential Applications of Fullerene Functionalized Molecular Glasses**

Fullerenes functionalized with methylaminotriazine glasses could potentially facilitate the process of thin film deposition and pave the way to different applications. Besides photovoltaic cells, another potential application is the fabrication of LED devices which requires transparent and conductive films.<sup>1</sup> In

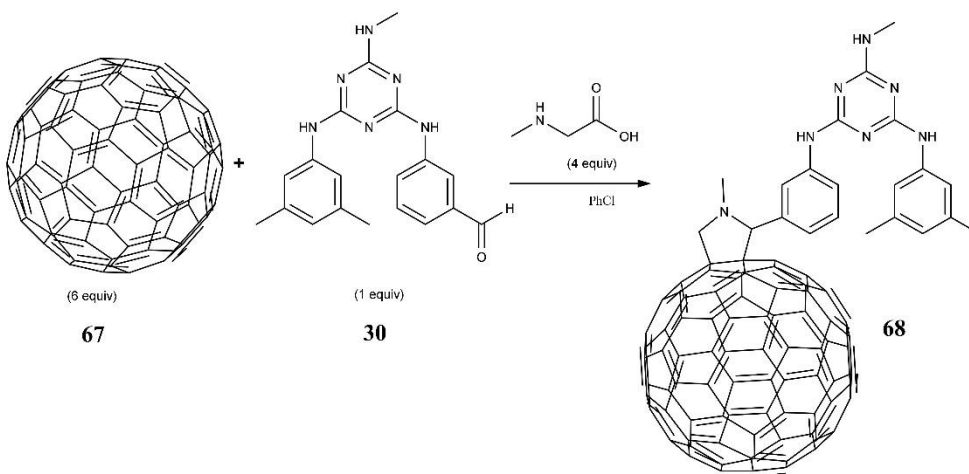
addition, these candidates are promising for the fabrication of electronic components which are the most appealing applications for thin film deposition.<sup>1</sup>

### 3.2. Results and Discussion

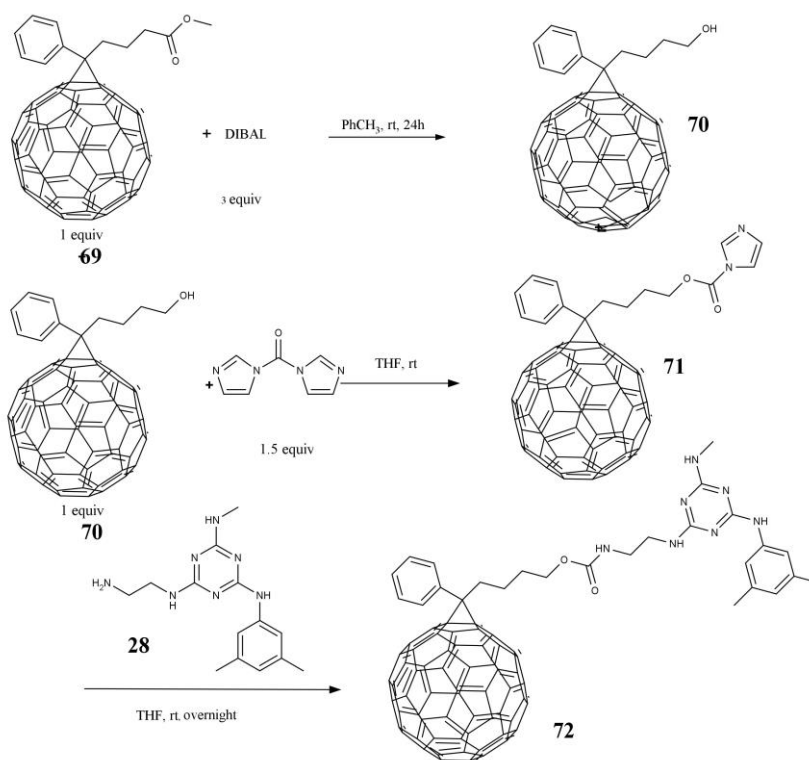
The synthetic procedures attempted to synthesize fullerene-functionalized molecular glasses are presented in Schemes 15-17.



Scheme 15: Synthesis of compound **66**.



Scheme 16: Synthesis of compound **68**.



Scheme 17: Synthesis of compound **72**.

### 3.2.1. Synthesis and Characterization

The synthetic routes attempted for candidates **66**, **68** and **72** are presented in Schemes 15-17. The procedure envisaged for compounds **66** and **68** was similar: the reaction involves the nucleophilic addition of commercially available sarcosine on the carbonyl group of glass **30** which involved formation of an iminium ion followed by decarboxylation to give an azomethine ylide which then reacts with the fullerene via a 1,3-dipolar cycloaddition reaction to obtain the desired product (Schemes 15 and 16). As PCBM is already substituted and possesses an ester group capable of further functionalization, the synthetic route used for compound **72** involved three steps. In the first step, the ester group of PCBM was reduced to the corresponding alcohol by diisobutylaluminum hydride (DIBAL). Next, the hydroxy group on intermediate **70** was reacted with N,N-carbonyldiimidazole to yield oxycarbonylimidazole **71**, which was then reacted with amino-substituted glass **28** in an attempt to make final product **72**, in a fashion similar to the synthesis of glass **31** from Disperse Red 1. However, as the resulting products were only slightly soluble in most organic solvents, purification and characterization proved extremely difficult.

Compound **66** gave the desired mass when characterized by HRMS. However, in the corresponding  $^1\text{H}$  NMR spectrum, extra peaks were observed in addition to the desired peaks for all fullerene products. Also, due to the low solubility of final products, the obtained peaks were broad and overlapped with other peaks. In order to get a proper  $^1\text{H}$  NMR spectrum with defined peaks, the compounds were purified by preparative TLC. However, the identity and purity of the product could still not be confirmed, as the NMR spectra showed several peaks unrelated to the expected products. Figures 19-22 show  $^1\text{H}$  NMR spectra for compound **66** and **72** before and after purification on preparative TLC plate.

### 3.3. Experimental

#### 3.3.1. Materials and Equipment

The materials used in attempted syntheses, sarcosine, DIBAL (diisobutylaluminum hydride), CDI (carbonyldiimidazole) and solvents (toluene, chlorobenzene, THF (tetrahydrofuran), DCM (dichloromethane), triethylamine, dehydrated solvents) were purchased from commercial sources and used without further purification.  $\text{C}_{60}$ ,  $\text{C}_{70}$  and PCBM (phenyl- $\text{C}_{61}$ -butyric acid methyl ester) were graciously donated by Solaris Chem, Inc. The process of purification was tried with silica gel (SiliaFlash P60 grade, SiliCycle) and TLC plates (SiliCycle). Compound **70**, aldehyde glass **30** and amino glass **28** were prepared according to a literature procedure.<sup>21, 71, 25</sup>

#### 3.3.2. Synthesis

The main part of this section involves the synthesis procedure of three fullerene functionalized molecular glasses. The synthetic routes of the targets (**66**, **68**, **72**) are depicted in Schemes 15-17. The starting materials were either commercially available or synthesized according to literature procedures.

##### 3.3.2.1. Attempted Synthesis of Compound **66**

In a round bottom flask equipped with a magnetic stir bar, chlorobenzene (300 mL) was degassed by sparging with  $\text{N}_2$  gas for 20 min. Next, fullerene- $\text{C}_{60}$  (6.013 g, 8.352 mmol), sarcosine (0.494 g, 5.568 mmol) and 2-methylamino-4-methylamino-6-(3-formylphenylamino)-1,3,5-triazine (0.485 g, 1.392 mmol) were added and the resulted solution was refluxed overnight under  $\text{N}_2$  atmosphere (Scheme 15). The solvent was removed under reduced pressure and THF (100 mL) was added to dissolve the product. The remaining fullerene- $\text{C}_{60}$  was recovered by filtration and washed with water and ethanol to remove any unreacted starting materials. THF was removed under vacuum and the desired product was washed with water and

ethanol. The product was filtered on a short silica pad with DCM/NEt<sub>3</sub> (98:2) as eluent. An analytical sample was further purified by preparative TLC using THF/hexanes (2:5) as eluent but gave an intractable mixture of products.

### 3.3.2.2. Attempted Synthesis of Compound 68

Chlorobenzene (15 mL) was degassed by sparging with N<sub>2</sub> gas for 20 min in a round bottom flask equipped with a magnetic stir bar. Fullerene-C<sub>70</sub> (0.2 g, 0.237 mmol), sarcosine (0.014 g, 0.158 mmol) and 2-methylamino-4-methylamino-6-(3-formylphenylamino)-1,3,5-triazine (0.013 g, 0.039 mmol) were added and the resulted solution was refluxed overnight under N<sub>2</sub> atmosphere (Scheme 16). The solvent was removed under reduced pressure and THF (10 mL) was added to dissolve the product. Remaining fullerene-C<sub>70</sub> was recovered by filtration and washed with water and ethanol to remove any unreacted starting materials. THF was removed under vacuum and the desired product was washed with water and ethanol. The crude product was filtered on a short silica pad using DCM/NEt<sub>3</sub> (98:2) as eluent. An analytical sample was further purified by preparative TLC using THF/hexanes (2:5) as eluent but gave an intractable mixture of products.

### 3.3.2.3. Attempted Synthesis of Compound 72

In a round bottom flask equipped with a magnetic stir bar, toluene (240 mL) was degassed by sparging with N<sub>2</sub> gas for 20 min. PCBM (0.810 g, 0.889 mmol) was dissolved in toluene followed by the dropwise addition of DIBAL (2.0 mL, 1 M solution in hexane). The mixture was stirred at room temperature for 24 h. In order to quench the reaction, 25 mL of saturated NH<sub>4</sub>Cl solution was added and the mixture was extracted with brine (3 x 250 mL). The toluene layer was dried over Na<sub>2</sub>SO<sub>4</sub> and the solvent was removed under reduced pressure to yield 0.991 g crude product **70**. In the second step, **70** (0.906 g, 1.026 mmol) was dissolved in dry THF (40 mL) and added dropwise to a suspension of CDI (0.248 g, 2.533 mmol) in dry THF (40 mL) in a dry round-bottomed flask equipped with a magnetic stirrer. The mixture was stirred at room temperature for 24 h. DCM (40 mL) was added and the mixture was extracted with water (3 x 50 mL). The organic layer was dried using anhydrous Na<sub>2</sub>SO<sub>4</sub> and evaporated under reduced pressure to afford 1.11 g product **71**. In the third step of the reaction, **71** (1.11 g, 1.133 mmol) was dissolved in THF (15 mL) followed by the addition of amino-substituted glass **28** (0.651 g, 2.26 mmol) and the resulted mixture was refluxed 18 h. After the reaction mixture was cooled down to room temperature, DCM (15 mL) was added, and the mixture was washed successively with 1M HCl (20 mL) and water (20 mL). The precipitate was filtered and washed with water. Next, the filtrate was dissolved in THF/DCM and washed with saturated aqueous NaHCO<sub>3</sub> and water. The organic layer was dried using anhydrous Na<sub>2</sub>SO<sub>4</sub> and evaporated under reduced pressure. The product was

washed with acetone to remove impurities. An analytical sample was further purified by preparative TLC using THF as eluent.

### **3.4. Summary**

The synthesis of molecular glasses functionalized with fullerene derivatives was attempted, however the low solubility of the products made the process of purification and analysis challenging, and the final products could not be obtained in pure form, and thus their identities could not be properly confirmed. The solution would be to design an improved plan to alter the structure of the candidates to increase the solubility in organic solvents. One synthetic option to modify the properties of products consists in adding alkyl chains to the skeleton of the glass. This would increase the solubility of products in common solvents and simplify the process of purification and characterization. Another option would be to functionalize the starting materials  $C_{60}$  and  $C_{70}$  with a functional group that can easily be bonded to a glass. This would ensure that the precursor could be properly purified and characterized.

## 3.5. Appendix

### 3.5.1. NMR Spectra

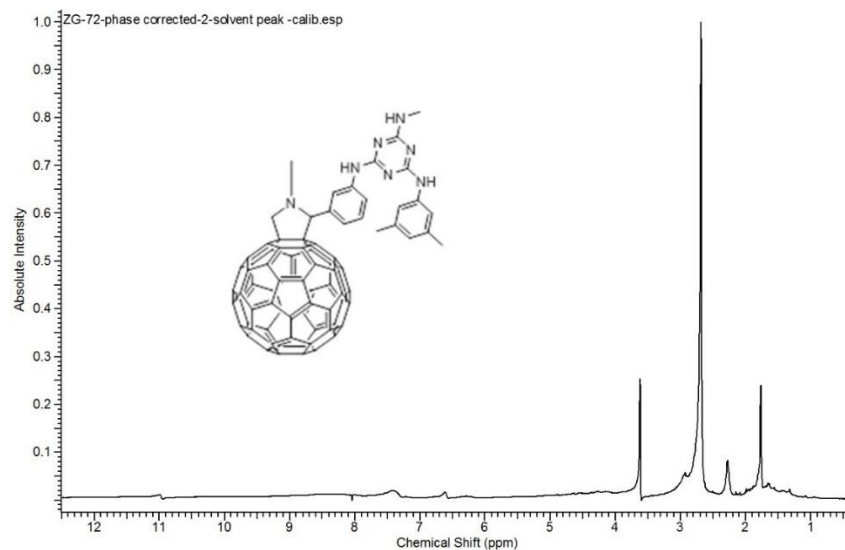


Figure 19:  $^1\text{H}$  NMR spectrum of compound **66** in THF, 400 MHz, before purification on preparative TLC plate.

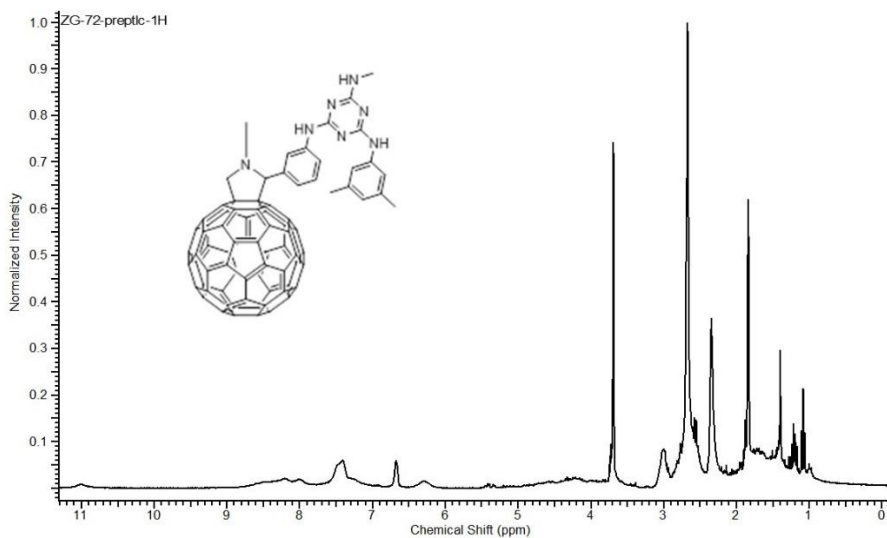


Figure 20:  $^1\text{H}$  NMR spectrum of compound **66** in THF, 400 MHz, after purification on preparative TLC plate.

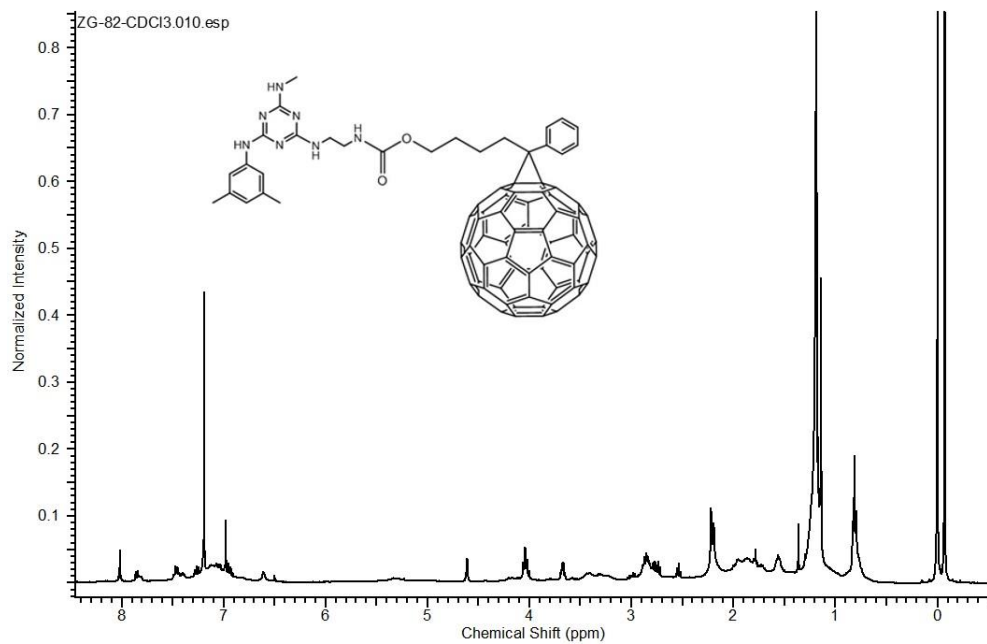


Figure 21:  $^1\text{H}$  NMR spectrum of compound **72** in THF, 400 MHz, before purification on preparative TLC plate.

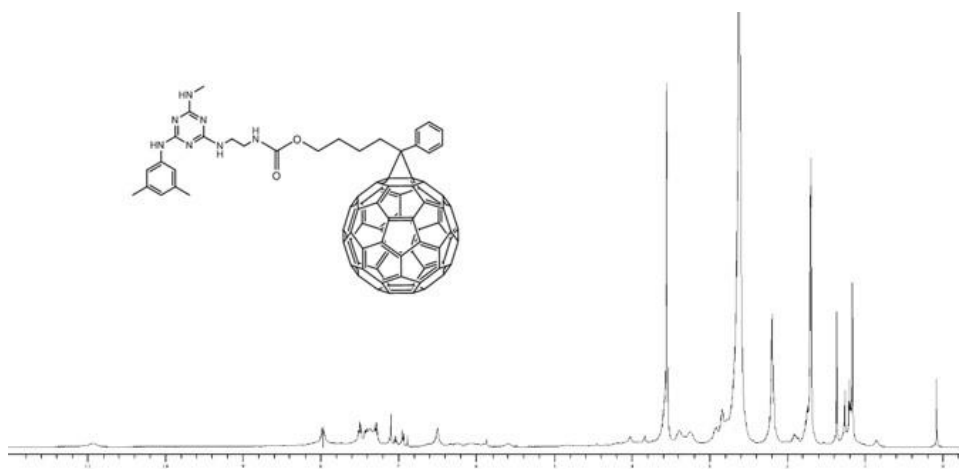


Figure 22:  $^1\text{H}$  NMR spectrum of compound **72** in THF, 400 MHz, after purification on preparative TLC plate.

## 4 Conclusion and Future Goals

The main aim of this thesis was to synthesize two series of functionalized molecular glasses, PDI and fullerene derivatives functionalized with mexylaminotriazine glasses. Chapter 1 provides a general introduction to molecular glasses and their applications. In chapter 2, the main goal was the synthesis of PDI functionalized mexylaminotriazine glasses and the investigation of their optical, thermal and photovoltaic properties. Chapter 3 describes the attempted synthetic procedures for fullerene-functionalized mexylaminotriazine glasses and their potential applications in electronic fields.

The first scientific part of this dissertation, chapter 2, was concerned with developing PDI-based glasses. A series of PDI dyes functionalized with mexylaminotriazine units have been synthesized which exhibit excellent glass forming ability and are soluble in common organic solvents. In addition, the candidates were shown to be capable of uniform thin film formation and absorb strongly in the visible range which make them promising candidates as optical or optoelectronic materials.

The synthesized glass-functionalized PDI samples have been studied as electron acceptors in OPV cells and promising results have been achieved. However, such results were obtained from preliminary tests and will be improved by optimization of PDI glass structure, spin coating conditions, choice of donor polymer and device fabrication. It is important to study the electronic and conducting properties of the PDI glasses in greater depth. This can be investigated by fabrication of devices such as light emitting diodes (OLEDs), thin film transistors and optimized organic photovoltaic cells.

The library of PDI functionalized glasses can be expanded by synthesizing other derivatives of PDI glasses. The remaining bromo group of compound **61** could be substituted with several other functional groups including cyano, alkoxy, aryloxy, alkylthio or arylthio groups. An alternative to the above would be synthesizing glass-functionalized PDI dyes without bay substituents. Instead of attaching the glass on the bay region, the mexylaminotriazine moiety would be located on one of the imide groups. The reaction conditions and purification process can be optimized by trying other literature procedures to improve the yield of the desired products.

Chapter 3 reported the synthetic procedures attempted to synthesize fullerene functionalized mexylaminotriazine glasses. The syntheses attempted were simple and straightforward to minimize purification steps. However, the crude products exhibited solubility problems and were thus difficult to purify, and even

after chromatography, the products were intractable by NMR spectroscopy. Modification of the structure of the methylaminotriazine units might improve the solubility.

One option to improve solubility and facilitate characterization, would be adding alkyl chains to the structure of the glass to make it more soluble in low polarity solvents. This would facilitate the purification and characterization process. Another solution to solve the problem is to attach a functional group to the fullerene followed by a reaction with the desired glass. This way, a precursor that is easy to purify and characterize could be obtained first and then reacted with the glass in an efficient step. Although the procedure would involve an additional synthetic step, the reaction with the glass would be performed with a pure functionalized product rather than with the fullerene itself.

The opportunity for the use of high performance organic thin films in modern electronic devices such as photovoltaic cells is expanding rapidly based on PDI and fullerene based semiconductors. In addition to fullerene and PDI families, other promising small molecules for the fabrication of high-performance photovoltaic cells are phthalocyanines such as CuPc, thiophenes and tris(8-hydroxyquinolino)aluminium (Alq<sub>3</sub>). However, such candidates are not capable of amorphous phase formation. In order to obtain high performance photovoltaic cells, mentioned candidates could be functionalized with methylaminotriazine glasses to impart glass forming ability on the linked moiety.

We hope that the research presented here will support with the incorporation of glass functionalized fullerene and PDI derivatives into other optoelectronic processes, in addition to organic photovoltaic cells.

## Bibliography

- 1) Schuegraf, K. *Handbook of Thin Film Deposition Processes and Techniques Principles, Methods, Equipment and Applications*. 2<sup>nd</sup> edition; Noyes: New York, 1988.
- 2) Shirota, Y. *J. Mater. Chem.* **2005**, *15*, 75–93.
- 3) Govender, K.; Boyle, D.; Kenway, P.; O'Brien, P. *J. Mater. Chem.* **2004**, *14*, 2575–2591.
- 4) Wuest, J.; Lebel, O.; *Tetrahedron*. **2009**, *65*, 7393–7402.
- 5) Tilley, R. *Understanding Solid*. Willey: West Sussex, 2004.
- 6) Yu, L. *Adv. Drug Deliv. Rev.* **2001**, *48*, 27–42.
- 7) Seo, J.; Oh, J.; Kwon, H.; Kim, H.; Hwang, Y. *American Institute of Physics*. **2006**, pp 37-45.
- 8) Crowe, L.M.; Reid, D.S.; Crowe, J.H.; *Biophys J.* **1996**, *71*, 2087-2093.
- 9) Slade, L.; Levine, H.; Reid, D. S.; *Crit. Rev. Food Sci. Nutr.* **1991**, *30*, 115-360.
- 10) Zotov, N. *J. Non-Cryst. Solids*. **2003**, *323*, 1–6.
- 11) Shirota, Y. *J. Mater. Chem.* **2000**, *10*, 1-25.
- 12) Lebel, O.; Maris, T.; Perron M. E.; Demers, E.; Wuest, J. D. *JACS*. **2006**, *128*, 10372-10373.
- 13) Nishimura, K.; Kobata, T.; Inada H.; Shirota, Y. *J. Mater. Chem.* **1991**, *1(5)*, 897-898.

- 14) Higuchi, A.; Ohnishi, K.; Nomura, S.; Inada H.; Shirota Y. *J. Mater. Chem.* **1992**, *2*(10), 1109-1110.
- 15) Inada, H.; Shirota Y.; *J. Mater. Chem.* **1993**, *3*(3), 319-320.
- 16) Kinoshita, M.; Kita, H.; Shirota, Y. *Adv. Funct. Mater.* **2002**, *12*, 780-786.
- 17) Wang, S.; Oldham, E. J.; Raymond, A.; Hudack, R. A.; Bazan, G.C.; *J. Am. Chem. Soc.* **2000**, *122*, 5695-5709.
- 18) Kimura, M.; Kuwano, S.; Sawaki, Y.; Fujikawa, H.; Noda, K.; Taga Y.; Takagi K.; *J. Mater. Chem.* **2005**, *15*, 2393-2398.
- 19) Geng, Y.; Katsis, D.; Culligan, SW.; Ou, J. J.; Chen, S.; Rothberg, L. J. *Chem. Mater.* **2002**, *14*, 463-470.
- 20) Plante, A.; Mauran, D.; Carvalho, S. P.; J. Y. S. Danny Page´, J. Y. S. D.; Pellerin, C.; O Lebel, O. *J. Phys. Chem. B* **2009**, *113*, 14884-14891.
- 21) Eren, R. N.; Plante, A.; Meunier, A.; Laventure A.; Huang Y.; Briard, J. G.; Creber, K. J.; Pellerin, C.; Soldera, A.; Lebel, O. *Tetrahedron.* **2012**, *68*, 10130-10144.
- 22) Laventure, A.; Soldera, A.; Pellerin C.; Lebel O. *New J. Chem.*, **2013**, *37*, 3881-3889.
- 23) Wuest, J. D.; Lebel. O. *Tetrahedron.* **2009**, *65*, 7393-7402.
- 24) O. Lebel, Molecular Glasses with Functionalizable Groups, Can. Patent. Appl. 2762434, 2001.
- 25) Meunier, A.; Lebel, O.; *Org. Lett.* **2010**, *12*, 1896-1899.
- 26) Kirby, R.; Sabat, R. G.; Nunzi, J. M.; Lebel, O. *J. Mater. Chem. C*, **2014**, *2*, 841-847.
- 27) Hancock, B. C.; Zografis, G. *Int. J. Pharm.* **1997**, *86*, 1-12.

- 28) Craig, Q. M.; Royall, P. G.; Kett V. L.; Hopton, M. L. *Int. J. Pharm.* **1999**, *179*, 179–207.
- 29) Shirota, Y.; Kageyama H. *Chem. Rev.* **2007**, *107*, 953–1010.
- 30) Shirota, Y.; Kobata, T.; Noma, N. *Chem. Lett.* **1989**, 1145-1148
- 31) Ishikawa, W.; Inada, H.; Nakano, H.; Shirota, Y. *Chem. Lett.* 1991, 1731-1734.
- 32) Oyston, S.; Wang, C.; Hughes, G.; Batsanov, A. S.; Perepichka, I. F.; Bryce, M. R.; Ahn, J. H.; Pearson J. H.; Pearson, C.; Petty, M. C. *J. Mater. Chem.* **2005**, *15*, 194-203.
- 33) Kido, J.; Hongawa, K.; Okuyama, K.; Nagai, K. *Appl. Phys. Lett.* **1993**, *63*, 2627-2629.
- 34) Zhou, X.; Pfeiffer, M.; Huang, J. S.; Blochwitz-Nimoth, J.; Qin, D. S.; Werner, A.; Drechsel, J.; Maennig, B.; Leo, K. *Appl. Phys. Lett.* **2002**, *81*, 922-924.
- 35) Naka, S.; Okada, H.; Onnagawa, H.; Tsutsui, T. *Appl. Phys. Lett.* **2000**, *76*, 197-199.
- 36) Jandke, M.; Strohriegl, P.; Berleb, S.; Werner, E.; Brütting, W. *Macromolecules* **1998**, *31*, 6434-6443.
- 37) Noda, T.; Shirota, Y. *J. Am. Chem. Soc.* **1998**, *120*, 9714-9715.
- 38) Palilis, L. C.; Makinen, A. J.; Uchida, M.; Kafafi, Z. H. *Appl. Phys. Lett.* **2003**, *82*, 2209-2211.
- 39) Nunzi, J. M. *C. R. Physique.* **2002**, *3*, 523–542.
- 40) Hong, Z. R.; Lee, C. S.; Lee, S. T.; Li, W. L.; Shirota, Y. *Appl. Phys. Lett.* **2002**, *81*, 2878-2880.
- 41) Xue, J.; Uchida, S.; Rand, B. P.; Forrest, S. R. *Appl. Phys. Lett.* **2004**, *84*, 3013-3015.

- 42) Xue, J.; Rand, B. P.; Uchida, S.; Forrest, S. R. *Adv. Mater.* **2005**, *17*, 66-71.
- 43) Chu, C.-W.; Shao, Y.; Shrotriya, V.; Yang, Y. *Appl. Phys. Lett.* **2005**, *86*, 243506.
- 44) Yoo, S.; Domercq, B.; Kippelen, B. *Appl. Phys. Lett.* **2004**, *85*, 5427.
- 45) Zen, A.; Bilge, A.; Galbrecht, F.; Alle, R.; Meerholz, K.; Grenzer, J.; Neher, D.; Scherf, U.; Farrell, T. *J. Am. Chem. Soc.* **2006**, *128*, 3914-3915.
- 46) Ponomarenko, S. A.; Kirchmeyer, S.; Elschner, A.; Alpatova, N. M.; Halik, M.; Klauk, H.; Zschieschang, U.; Schmid, G. *Chem. Mater.* **2006**, *18*, 579-586.
- 47) De Angelis, F.; Cipolloni, S.; Mariucci, L.; Fortunato, G. *Appl. Phys. Lett.* **2005**, *86*, 203505.
- 48) Malenfant, P. R. L.; Dimitrakopoulos, C. D.; Gelorme, J. D.; Kosbar, L. L.; Graham, T. O. *Appl. Phys. Lett.* **2002**, *80*, 2517-2519.
- 49) Waldauf, C.; Schilinsky, P.; Perisutti, M.; Hauch, J.; Brabec, C. *J. Adv. Mater.* **2003**, *15*, 2084-2088.
- 50) Sonntag, M.; Kreger, K.; Hanft, D.; Strohrriegl, P.; *Chem. Mater.* **2005**, *17*, 3031-3039.
- 51) Durr, H.; Lament, H. B.; *PHOTOCHROMISM Molecules and Systems*, Elsevier: Amsterdam, 2003.
- 52) Utsumi, H.; Nagahama, D.; Nakano H.; Shirota, Y.; *J. Mater. Chem.* **2002**, *12*, 2612-2619.
- 53) Negahama, D.; Nakano, H.; Shirota, Y.; *J. Photopolym. Sci. Technol.* **2008**, *21*, 755-757.
- 54) Mack, C. A.; *Fundamental Principles of Optical Lithography: The science of Microfabrication*. Wiley: London, 2007.

- 55) Yoshiiwa, M.; Kageyama, H.; Shirota Y. *Appl. Phys. Lett.* **1996**, *69*, 2605-2607.
- 56) Chang, S. W.; Ayothi, R.; Bratton, D.; Yang, D.; Felix, N.; Cao, H. B.; Deng, H.; Ober, C. K.; *J. Mater. Chem.* **2006**, *16*, 1470–1474.
- 57) Settels, V.; Liu, W.; Pflaum, J.; Fink, R. F.; Engels B.; *J. Comput. Chem.* **2012**, *33*, 1544–1553.
- 58) Kaur, B.; Bhattacharya, S. N.; Henry D. J. *Dyes and Pigments*, **2013**, *99*, 502-511.
- 59) Zhang, X.; Lu, Z.; Ye, L.; Zhan, C.; Hou, J.; Zhang, S.; Jiang, B.; Zhao, Y.; Huang, J.; Zhang, S.; Liu, Y.; Shi, Q.; Liu, y.; Yao, J. *Adv. Mater.* **2013**, *25*, 5791–5797.
- 60) Angadi, M. A.; Gosztola, D.; Wasielewski, M. R. *Mater. Sci. Eng.* **1999**, *63*, 191-194.
- 61) Wurthner, F.; Stepanenko, V.; Chen, Z.; Saha-Moller, C. R.; Kocher, N.; Stalke, D.; *J. Org. Chem.* **2004**, *69*, 7933-7939.
- 62) Law, K.Y. *Chem. Rev.* **1993**, *93*, 449-486.
- 63) Li, F. M.; Nathan, A.; Wu, Y.; Ong, B. S. *Organic Thin Film Transistor Integration*, Wiley: Weinheim, 2011.
- 64) Wurthner, F. *Chem. Commun.* **2004**, 1564-1579.
- 65) Kozma, E.; Catellani, M. *Dyes and Pigments*, **2013**, *98*, 160-179
- 66) Martin, N.; Giacalone, F. *Fullerene Polymers Synthesis, Properties and Applications* Wiley: Weinheim, 2009.
- 67) Haddon, R. C.; Perel, A. S.; Morris, R. C.; Palstra, T. T. M.; Hebard, A. F.; Fleming, R. M. *Appl. Phys. Lett.* **1995**, *67*, 121.

- 68) Brabec, C.; Dyakonov, V.; Scherf U.; *Organic Photovoltaics Materials, Device Physics, and Manufacturing Technologies*. Wiley: Weinheim, 2008.
- 69) Eklund, P. C.; Rao, A. M.; *Fullerene Polymers and Fullerene Polymer Composites*. Springer-Verlog: Berlin, 1999.
- 70) Yasuda, T.; Fujita, K.; Tsutsui, T.; Geng, Y.; Culligan, S. W.; Chen, S. H. *Chem. Mater.* **2005**, *17*, 264.
- 71) Zhanga, W. B.; Hea, J.; Donga X.; Wanga C. L.; Hui L.; Teng, F.; Li, X.; Wesdemiotis, C.; Quirka, R.P.; Chenga, S.Z.D. *Polymer*, **2011**, *52*, 4221-4226.
- 72) Chien, C.; Lin, C.C.; Watanabe, M.; Lin, Y. D.; Chao, T.; Chiang,T.; Huang, X.; Wen, Y.; Tu,C.; Sun. C.; Chow. T. *J. Mater. Chem.* **2012**, *22*, 13070-13075.

